Photosynthesis Research
https://doi.org/10.1007/s11120-018-0588-7

ORIGINAL ARTICLE

Low temperature induced modulation of photosynthetic induction in non-acclimated and cold-acclimated *Arabidopsis thaliana*: chlorophyll *a* fluorescence and gas-exchange measurements

Kumud B. Mishra[1,2] · Anamika Mishra[1] · Jiří Kubásek[1] · Otmar Urban[1] · Arnd G. Heyer[3] · Govindjee[4]

Received: 26 March 2018 / Accepted: 24 September 2018

Abstract

Cold acclimation modifies the photosynthetic machinery and enables plants to survive at sub-zero temperatures, whereas in warm habitats, many species suffer even at non-freezing temperatures. We have measured chlorophyll *a* fluorescence (ChlF) and CO_2 assimilation to investigate the effects of cold acclimation, and of low temperatures, on a cold-sensitive *Arabidopsis thaliana* accession C24. Upon excitation with low intensity (40 µmol photons m^{-2} s^{-1}) ~ 620 nm light, slow (minute range) ChlF transients, at ~ 22 °C, showed two waves in the SMT phase (S, semi steady-state; M, maximum; T, terminal steady-state), whereas CO_2 assimilation showed a linear increase with time. Low-temperature treatment (down to − 1.5 °C) strongly modulated the SMT phase and stimulated a peak in the CO_2 assimilation induction curve. We show that the SMT phase, at ~ 22 °C, was abolished when measured under high actinic irradiance, or when 3-(3, 4-dichlorophenyl)-1, 1- dimethylurea (DCMU, an inhibitor of electron flow) or methyl viologen (MV, a Photosystem I (PSI) electron acceptor) was added to the system. Our data suggest that stimulation of the SMT wave, at low temperatures, has multiple reasons, which may include changes in both photochemical and biochemical reactions leading to modulations in non-photochemical quenching (NPQ) of the excited state of Chl, "state transitions," as well as changes in the rate of cyclic electron flow through PSI. Further, we suggest that cold acclimation, in accession C24, promotes "state transition" and protects photosystems by preventing high excitation pressure during low-temperature exposure.

Keywords Low-temperature effect · Cold acclimation · Chlorophyll fluorescence transients · Slow SMT fluorescence phase · Gas-exchange measurements · State transition · 3-(3, 4-dichlorophenyl)-1, 1- dimethylurea · Methyl viologen

Abbreviations

A	CO_2 assimilation rate
AC	Cold acclimated
A_{gross}	Gross CO_2 assimilation rate
A_{max}	Maximum CO_2 assimilation rate under saturating light
Chl *a*	Chlorophyll *a*
ChlF	Chlorophyll *a* fluorescence
DCMU (also called diuron)	3-(3, 4-dichlorophenyl)-1, 1- dimethylurea
F'_m	Maximum fluorescence intensity during actinic light exposure
$F''_m(t)$	Maximum fluorescence intensity during dark-relaxation
F683	Fluorescence emission band, with a maximum at 683 nm
F735	Fluorescence emission band, with a maximum at 735 nm

Five of us (KBM, AM, JK, OU, and AGH) pay tribute to three pioneers of Photosynthesis Research, Agepati S. Raghavendra (carbon reactions, specifically for C4 photosynthesis), William A. Cramer (bioenergetics, specifically for biochemistry and biophysics of cytochromes), and Govindjee (primary photochemistry and electron transport, specifically for the unique role of bicarbonate in Photosystem II; also a co-author of this manuscript), for their contributions and commendable leadership in photosynthesis research.

Electronic supplementary material The online version of this article (https://doi.org/10.1007/s11120-018-0588-7) contains supplementary material, which is available to authorized users.

✉ Kumud B. Mishra
mishra.k@czechglobe.cz

Extended author information available on the last page of the article

Published online: 10 October 2018

F_m	Maximum fluorescence when the (plasto) quinone Q_A is fully reduced
F_O	Minimum fluorescence when Q_A is fully oxidized
F_P	Fluorescence intensity at the P level
F_{M1}	Fluorescence intensity at peak M_1
F_{M2}	Fluorescence intensity at peak M_2
F_T	Terminal steady-state fluorescence
F_v	Maximum variable ChlF ($F_m - F_O$)
F_v/F_m	Equivalent to maximum quantum yield of PSII photochemistry
IS_{60}	Induction state of A at 60 s after illumination, expressed as a percent of A_{max}
IT_{50}	Induction time required to reach 50% of A_{max}
k (k^{-1})	Rate constant (inverse of rate constant) [of the P-to-S phase]
LHCs	Light-harvesting complexes
M_1, M_2	First and second maxima after peak P (F_P) in the SMT phase of ChlF transient
MV	Methyl viologen
NAC	Non-acclimated
NPQ	Non-photochemical quenching (of the excited state of Chl *a*)
PQ	Plastoquinone
PSI	Photosystem I
PSII	Photosystem II
Q_A, Q_B	The first and the second (plasto) quinone acceptors of electrons in the reaction center of PSII
R_{FD}	Fluorescence decrease ratio defined as F_D/F_T, where $F_D = F_P - F_T$
RuBP	Ribulose-1,5-bisphosphate
SMT	Slow phase of chlorophyll *a* fluorescence transient (where S is semi steady-state, M is a maximum and T is terminal steady-state)
t_{Fp}	Time required to reach P (F_P) level
t_{M1}	Time required to reach M_1 level of ChlF transient
t_{M2}	Time required to reach M_2 level of ChlF transient
t_{50}	Time required for 50% decline from P (F_P) to the S level
ΔpH	pH difference across the thylakoid membrane
$\Phi_{f,d}$	Quantum yield of "constitutive" thermal dissipation (d) and fluorescence (f)
Φ_{NPQ}	Quantum yield of "regulated" non-photochemical quenching
Φ_{PSII}	Quantum yield of PSII photochemistry
Φ_{qE}	Quantum yield of "fast" energy (E) dependent quenching
Φ_{qI}	Quantum yield of photoinhibition (I) quenching of Chl fluorescence
Φ_{qT}	Quantum yield of state-transition (T) quenching of Chl fluorescence, during *State I* (high fluorescence) to *State II* (low fluorescence)

Introduction

Low temperature, classified as chilling (0 °C < T < 15 °C) or freezing (T < 0 °C), is a major factor in limiting growth, survival and geographical distribution of plants (Berry and Björkman 1980; Allen and Ort 2001; Hasdai et al. 2006). Plants adapted to warm habitats are highly susceptible to cold (prolonged exposure to low temperature, or a sudden temperature drop). Under such conditions, there is a decrease in the yield, or a complete failure, of important agricultural crops (Leegood and Edwards 1996). In cold habitats, however, plants overcome the effects of low temperature, and survive even at sub-zero temperatures. The gain in cold tolerance is due to a highly complex process of cold acclimation (Guy 1990; Thomashow 2010; Crosatti et al. 2013), activated by dynamic interaction between the exposure to non-freezing temperatures (0–10 °C) and light (Wanner and Junttila 1999; Smallwood and Bowles 2002; Franklin and Whitelam 2007; Catalá et al. 2011). It is well known that the capacity for cold acclimation is dependent on the latitudinal range of habitats in natural accessions of *Arabidopsis thaliana* (hereafter *Arabidopsis*) (Hannah et al. 2006; Mishra et al. 2011, 2014; Lukas et al. 2013). However,

mechanisms underlying cold acclimation as well as regulatory steps controlling re-adjustment of the physiological homeostasis at low temperatures remain poorly understood. This is particularly true for responses of photosynthetic reactions, and associated metabolic pathways, when plants experience a sudden drop in temperature. Understanding the underlying biophysical, biochemical, and physiological processes is crucial for elucidating how photosynthesis functions at these temperatures, particularly for the development of breeding strategies (Ort et al. 2015).

Plants have evolved several regulatory strategies for protecting their photosystems while optimizing efficiency under unfavorable environmental stimuli. In general, low temperature leads to a decline in membrane fluidity that inhibits electron transport by restricting mobilization of hydrophobic proteins, redox homeostasis, and the repair cycle of D1 protein (Aro et al. 1990; Allen and Ort 2001). Low temperature affects the rate of enzymatic reactions of the Calvin–Benson cycle far more than the primary photophysical and photochemical processes, involved in light absorption, excitation energy transfer, and conversion of light energy into chemical energy, and, thus, there is the possibility of imbalance between the absorbed and the used light energy (Berry and Björkman 1980; Bernacchi et al. 2002; Ensminger et al. 2006; Sage and Kubien 2007; Horton 2012; Khanal et al. 2017). The decreased biochemical consumption of the products of photochemical reactions, i.e., NADPH and ATP, in the enzymatic reactions, in turn, creates a situation as if there is high irradiance, which may cause elevated excitation pressure (Öquist et al. 1987; Huner et al. 1998) and over-reduce the system (Endo et al. 2005). This stimulates several stress responses, e.g., increases in the cyclic electron transport around photosystem (PS) I (Endo et al. 2005), in the water–water cycle (Asada 1999), and production of damaging reactive oxygen species (Triantaphylidès and Havaux 2009) that may further result in photoinhibition (Allakhverdiev et al. 1997; Tyystjärvi 2013) of both PSI and PSII. The light-harvesting complexes (LHCs) of both photosystems must, therefore, dispose of potentially harmful absorbed energy by dissipating it as heat through photo-protective processes, such as non-photochemical quenching (NPQ) of the excited state of chlorophyll *a* (Chl *a*) (Demmig-Adams and Adams 2000; Müller et al. 2001; Ruban et al. 2007; Murchie and Niyogi 2011; Horton 2012; Demmig-Adams et al. 2014). Moreover, cold acclimation reduces the functional absorption cross section of PSII antenna to avoid over-excitation of the system (Huner et al. 1998; Khanal et al. 2017).

Adjustments in photosynthetic mechanisms in response to low temperatures can be probed in vivo through non-invasive and highly sensitive Chl *a* fluorescence (ChlF) measurements. ChlF induction kinetics, fluorescence emission spectra at room temperature and at 77 K, and their parameters have been successfully used to probe the effects of biotic as well as abiotic stress on photosynthetic reactions (Oxborough 2004; Papageorgiou and Govindjee 2004; Baker 2008; Malenovský et al. 2009; Kalaji et al. 2012; Goltsev et al. 2016; Mishra et al. 2016a; Stirbet et al. 2018). Application of saturation pulses on ChlF transient has been used for understanding the fate of absorbed energy into highly complex photochemical and non-photochemical processes. Efforts have been undertaken by several laboratories to extend the so-called "saturation pulse methods" for energy partitioning, for the evaluation of the quantum yield of various photochemical and non-photochemical processes (Cailly et al. 1996; Hendrickson et al. 2004; Kramer et al. 2004; Ahn et al. 2009; Guadagno et al. 2010; reviewed in Lazár 2015). Information on the quantum yield of various processes is also needed for a detailed understanding of the responses of the photosynthetic apparatus to environmental factors and acclimation. Nevertheless, ChlF methods have not been fully exploited for the in vivo analysis of photosynthetic responses to cold acclimation and low temperatures. However, attempts have already been made to use ChlF parameters for the screening of cold tolerance (Baker and Rosenqvist 2004; Ehlert and Hincha 2008; Mishra et al. 2011, 2014; Humplík et al. 2015) and for the investigation of certain metabolic effects on PSII integrity (Knaupp et al. 2011). The relative contributions of PSII and PSI, as measured through both ChlF induction and emission spectra, were found to change during cold exposure (Agati et al. 2000; Franck et al. 2002). By measurement of ChlF parameter, F_v/F_m, i.e., the ratio of variable to maximal fluorescence, which represents maximum quantum yield of PSII photochemistry, during cooling of detached leaves to the freezing temperature of ~ − 20 °C, Ehlert and Hincha (2008) and Knaupp et al. (2011) showed that damage to PSII occurs at temperatures below those causing damage to the plasma membrane. Usually, F_v/F_m is very stable at or near sub-zero temperatures (Pospíšil et al. 1998; Mishra et al. 2011), and its decline at lower temperatures might be due to freezing-induced severe dehydration stress (Hacker et al. 2008), which occurs probably by "blocking" of the reaction centers at lower temperatures (Pospíšil et al. 1998). Mishra et al. (2011) have measured ChlF transients in differentially cold-tolerant *Arabidopsis* accessions during progressive cooling (− 2 °C h^{-1}) and reported that low-temperature treatments stimulate slow (seconds to minute range) SMT fluorescence phase (for a review of this phase, see Papageorgiou and Govindjee 2011; also see Stirbet and Govindjee 2016). Although the presence of slow SMT phase in ChlF transients has been reported in various photosynthetic organisms (Papageorgiou et al. 2007; Papageorgiou and Govindjee 2011), yet, the mechanisms involved in the formation of SMT phase and its relation to photosynthetic processes at low temperature is not at all clear.

In order to better understand how photosynthetic processes and the SMT phase of ChlF induction are influenced by low temperatures, we have measured changes in slow ChlF transients, in the fluorescence emission spectra in the 650–780 nm range, and evaluated quantum yield of photochemical and non-photochemical quenching of the excited state of Chl *a*, at selected temperatures during controlled cooling from 22 °C down to − 1.5 °C, in non-acclimated (NAC) and cold-acclimated (AC) leaves of the cold-sensitive *Arabidopsis* accession C24 (Hannah et al. 2006). Further, we measured fluorescence emission spectra at 77 K, before and after low-temperature treatment at − 1.5 °C to access effects on "state changes" (Kaňa et al. 2012). In order to understand how the slow SMT phase of ChlF transient is formed, we have analyzed detached leaves that were vacuum infiltrated with the electron transport inhibitor, 3-(3,4-dichlorophenyl)-1,1-dimethylurea (DCMU), and a PSI electron acceptor, methyl viologen (MV). In addition, we have measured the induction of CO_2 assimilation (*A*) in intact NAC and AC C24 plant rosettes to investigate how low temperatures affect CO_2 assimilation. Here, we present new datasets that revealed photochemical as well as biochemical effects of low temperature on the modulation of SMT fluorescence phase and the importance of cold acclimation in regulation of photosynthetic processes at low temperatures.

Materials and methods

Plant material and growth conditions

Arabidopsis accession C24, originating from the Iberian Peninsula (see Schmid et al. 2003; Hannah et al. 2006), was grown, for four weeks, in GS90 soil and vermiculite (1:1). Three plants per 100-mm diameter pot were placed in a growth chamber [8-h fluorescent light (120 µmol photons m^{-2} s^{-1}; 22 °C)/16-h dark; 16 °C]. Then the plants were transferred to long day conditions (16-h light, 8-h dark), but kept under the same irradiance and the temperature regime. Plants were watered daily and fertilized every two weeks with standard nitrogen (N), phosphorus (P), and potassium (K) fertilizer. Six weeks after germination, half of the plants (24 in number) were transferred to a 4 °C chamber for cold acclimation (AC) for two weeks, whereas the non-acclimated (NAC) plants were kept at 22 °C (day) and 16 °C (night). All physiological measurements were made on 8-week-old NAC and AC plants. For measuring CO_2 assimilation rates of the whole rosettes, we used *Arabidopsis* plants as described above, but their seedlings (two weeks after germination) were transplanted in Ray Leach cone-type pots (140 mm long; 38 mm diameter; Stuewe & Sons Tangent, Oregon, USA) that were suitable to fit into a whole plant *Arabidopsis* chamber (6400-17; LI-COR Biosciences, USA).

Chlorophyll *a* fluorescence (ChlF) transients

For measuring ChlF transients, detached leaves, from both NAC and AC plants, were arranged on a black wooden plate, and their petioles were kept under drops of water. The HANDY chlorophyll fluorescence imaging system (Photon Systems Instruments, Brno, CZ) was set above the black plate with leaf samples inside a cooling device that was slowly cooled at a rate of − 2 °C h^{-1}, from 10 °C to − 2 °C. Cooling from 22 °C to 10 °C was accomplished within 1 h, and then the slow cooling (− 2 °C h^{-1}) down to − 2 °C was started. The cooling device was programmed to stop cooling at selected temperatures during the measurement. The temperatures in the vicinity of the detached leaves were measured by two sets of data loggers [DS1921 Thermocron, Maxim Integrated, San Jose (CA), USA], which monitored the temperature every five minutes. The fluorescence imaging system, used for measuring ChlF transients (Fig. 1), as described by Mishra et al. (2014), was equipped with four orange light (620 nm) emitting diode panels, programmed to generate 10-µs measuring flashes (~ 1 µmol photons m^{-2} s^{-1}; frequency: 19.63 Hz), saturating flashes of ~ 1800 µmol photons m^{-2} s^{-1}, and actinic light of selected intensity. Flashes of the light-emitting devices (LEDs) were synchronized with the opening of the electronic shutter of the charged-coupled device (CCD) camera (512 × 512 pixels, 12 bits). An optical dark red glass filter (RG695) was placed in front of the CCD camera to block the light of the LEDs. ChlF transients are usually measured after 20–30 min of dark adaptation (which is long enough to have all Q_A in the oxidized state); longer dark adaptation may inactivate several Calvin–Benson cycle enzymes; these changes also influence ChlF transients (see Mishra et al. 2016b). Thus, we programmed our imaging system to measure ChlF transients automatically at 30-min intervals during the cooling of the leaves from 22 °C to − 1.5 °C.

The experimental protocol for measuring ChlF transients (Fig. 1) began with the measurement of minimum (O, F_O) and maximum (F_m) fluorescence levels by exposing leaves, respectively, to the measuring and the saturating light flashes. After ~ 60-s dark adaptation, leaves were exposed to actinic irradiance [40 µmol photons m^{-2} s^{-1}] for about 8 min to measure the kinetics of the ChlF transient up to the terminal steady-state (F_T). At the end of the actinic illumination, a saturating flash was applied to probe the non-photochemical quenching [$NPQ = (F_m - F'_m)/F'_m$, where F'_m is the maximal fluorescence in light; Maxwell and Johnson 2000] and the effective quantum yield of PSII photochemistry [$\Phi_{PSII} = (F'_m - F_T)/F'_m$; Genty et al. 1989] of the leaves. Further, the fluorescence decrease ratio ($R_{FD} = F_D/F_T$, where, $F_D = F_P - F_T$, and F_P = intensity of florescence peak under actinic irradiance) was calculated. After the actinic light was switched off, a saturating flash was given after ~ 30 s

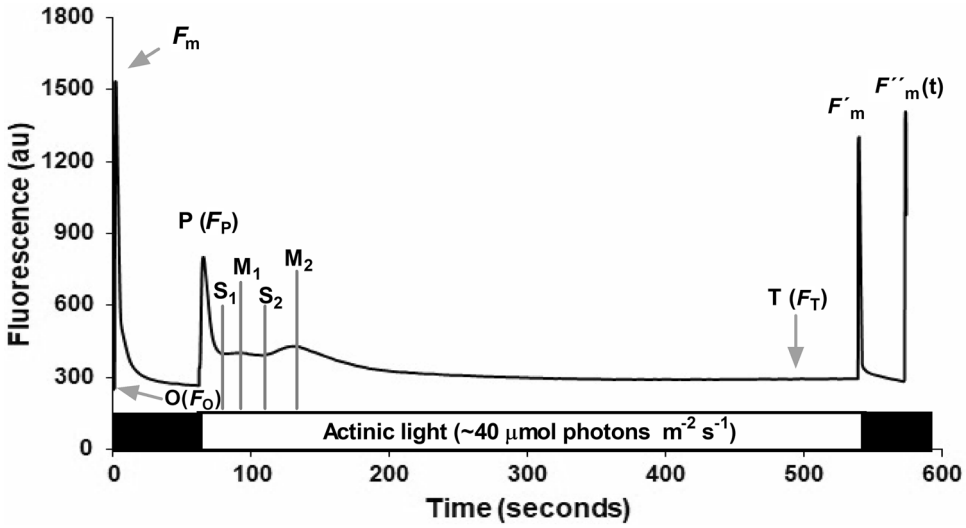

Fig. 1 Protocol for the measurement of chlorophyll *a* fluorescence (ChlF) transients, used in our experiments. Dark-adapted (20 min) leaves were used to first measure the minimum O (F_O) level with a weak 10-μs-long measuring light (620 nm, intensity, ~1 μmol photons m^{-2} s^{-1}), and then the maximum (F_m) level by exposing the sample to a saturating 620 nm light flash (~1800 μmol photons m^{-2} s^{-1}). After a 60-s dark period, leaves were exposed to 620 nm actinic irradiance (~40 μmol photons m^{-2} s^{-1}) for about 8 min to measure ChlF transient up to the (terminal) steady-state, "T" (F_T). At the end of the actinic light exposure, the same saturating flash (see above) was applied to measure the maximum fluorescence (F'_m) to evaluate the non-photochemical quenching (NPQ) of Chl *a* fluorescence, and the effective PSII quantum yield (Φ_{PSII}). After ~30-s dark period, another saturating flash was given to measure the relaxation of maximum fluorescence in dark F''_m(t). Note that the "O" (F_O) level is when Q_A in all active PSII reaction centers are assumed to be in the oxidized state; I is an inflection (not seen in this diagram); F_P ("P" for peak) is when Q_A in all active PSII reaction centers are assumed to be in the reduced state; S is for semi steady-state; M_1 and M_2 denote maxima for two peaks in the slow fluorescence phase; and T is for terminal steady-state, F_T. See Papageorgiou and Govindjee (2011) for further details

to measure the relaxation of maximum fluorescence in the dark, F''_m (t), for investigating the relaxation of the faster energy-dependent quenching (qE).

Quantum yield of photochemical and non-photochemical quenching processes

To estimate the quantum yields of photochemical and different types of non-photochemical processes using energy partitioning approach (Cailly et al. 1996; Hendrickson et al. 2004), ChlF transients of 20-min dark-adapted leaves of both the NAC and the AC plants were measured for about 15 min in the presence of actinic light; this was followed by the measurement of the dark-relaxation of the F'_m, F''_m(t), at several time intervals ranging from 2 to 1200 s, as used by Roháček et al. (2008). For further details on the measuring protocol, see Supplementary Fig. S1 (also see Roháček et al. 2008; Roháček 2010). We used here the equations given by Hendrickson et al. (2004) to quantify the partitioning of absorbed energy into the quantum yield of PSII photochemistry ($\Phi_{PSII} = (F'_m - F_T)/F'_m$; Genty et al. 1989), the quantum yield of "regulated" NPQ ($\Phi_{NPQ} = F_T/F'_m - F_T/F_m$; Cailly et al. 1996; cf. Lazár 2015), and the "non-regulated" NPQ composed of the sum of quantum yield of fluorescence and "constitutive" thermal dissipation ($\Phi_{f,d} = F_T/F_m$; Cailly et al. 1996; cf. Lazár 2015). Further, we analyzed the dark-relaxation kinetics of NPQ by non-linear regression of three exponentially decay components in order to resolve the half times of the following processes: ΔpH dependent (fast), excitation energy re-distribution due to state transition (medium), and photoinhibition (slow), as proposed by Walters and Horton (1991). We have used here methods given by Guadagno et al. (2010) for the calculation of quantum yields of the components of the regulatory NPQ, Φ_{NPQ}, i.e., Φ_{qE}, Φ_{qT}, and Φ_{qI}. For further detailed information, see Supplementary Fig. S1, the paper by Guadagno et al. (2010) and the review by Lazár (2015).

ChlF spectra measured during low-temperature treatment

Individual detached leaves were placed in a cooling device to measure ChlF emission spectra by FluorMax 3 spectrofluorometer (Jobin Yvon, Horiba Scientific, Japan). Leaves were illuminated with blue light (480 ± 0.5 nm, bandwidth 1 nm), obtained from a xenon lamp in the FluorMax instrument, and the steady-state ChlF emission spectra, after 5 min of illumination, were measured in the 640–780 nm range with an integration time of 0.5 s and a bandwidth of 1 nm. Both the excitation light (falling on the leaf surface)

and the fluorescence (emitted by the leaf) were remotely sensed through a fiber-optic bundle that was connected to the excitation spectrometer and the front-face detector of the FluorMax via F-3000 Fiber Optic Mount. The sample was cooled at 2 °C h^{-1}, the cooling was stopped at selected temperatures, and then the fluorescence emission spectra were measured.

Low-temperature (77 K) fluorescence spectra

In order to check if there was state change (*State I* has relatively higher PSII than PSI fluorescence), we measured 77 K (using liquid nitrogen) ChlF spectra of the control and low-temperature (− 1.5 °C)-treated detached leaf discs from NAC and AC *Arabidopsis* plants. Leaf discs were placed, in a closed translucent Dewar flask, at 77 K, on a specially designed metal probe. All the leaf discs used had equal size and their ChlF spectra were recorded by a spectrometer (SM9000, Photon Systems Instruments, Brno, CZ) following excitation with LED blue light ($\lambda = 470$ nm, $\Delta\lambda = 20$ nm).

Treatment with diuron (DCMU) and methyl viologen (MV)

Detached leaves of both NAC and AC *Arabidopsis* plants were vacuum infiltrated for 20 s, at a pressure of ~ 400 mbar, with 10 ml solutions of (i) Diuron, 3-(3,4-dichlorophenyl)-1,1- dimethylurea [DCMU, which inhibits electron transport from PSII to PSI by displacing Q_B in PSII (see Govindjee and Spilotro 2002 for the procedure)] or (ii) Methyl viologen [MV, which accepts electrons from PSI (Munday and Govindjee 1969)] at room temperature. Because of the low solubility of DCMU in water, we first dissolved it in ethanol and then made stock solutions. The final concentrations of the chemicals used were: 100 µM and 200 µM DCMU, and 100 µM and 500 µM MV. To compare results between the control and chemically treated samples, all the samples had 2% ethanol in the 10 ml solvent.

Gas-exchange measurements of CO_2 assimilation rate

Plants, grown in Ray Leach cone-type pots, were kept in a whole plant *Arabidopsis* chamber (6400-17, LI-COR Biosciences, Lincoln, NE, USA) that was air sealed; this chamber was attached to RGB (red–green–blue) light source (6400-18A, LI-COR Biosciences, USA) and a gas-exchange measuring system (LI-6400-18, LI-COR Biosciences, USA). The whole plant, fitted within its chamber, was placed in a freezer with controlled cooling (as described above), where 45-min dark-adapted rosettes were exposed to 300 µmol photons m^{-2} s^{-1} irradiance to measure CO_2 assimilation rates (A). Plant rosettes were provided with constant ambient CO_2 (385 ± 5 µmol CO_2 mol^{-1}) at 50 ± 5% air humidity. The time course of A was automatically recorded throughout the experiment, at 15-s intervals, during the dark adaptation period as well as during the light phase. The precise setting of temperature between 22 and 0 °C inside the assimilation chamber was achieved by using an integrated Peltier thermoelectric cooler of the LI-6400-18 type. The measured CO_2 assimilation rate was normalized per unit leaf area, which was estimated from the corresponding photographs of the rosettes with the help of Adobe Photoshop software (Adobe Systems Software, Dublin, Ireland). The gross CO_2 assimilation rate (A_{gross}) was estimated by adding the rate of respiration to the rate of net photosynthesis, the former measured during the dark phase of the assimilation curve. From the photosynthetic induction curves, we calculated the A after 15 min of light exposure (A_{max}), and at 60 s after illumination, expressed as a percentage of A_{max} (IS_{60}); in addition, we recorded the time required to reach 50% of A_{max} (IT_{50}). For further details, see Chazdon and Pearcy (1986) and Urban et al. (2008).

Tools for data analysis and statistical analysis

Image processing software integrated with the FluorCam (http://www.psi.cz) was used to process the "captured" fluorescence image sequences and to calculate the averaged fluorescence parameters over the whole leaf area. Specific features of Graphpad Prism Software, version 5 (GraphPad software, La Jolla, CA, USA), were used for a quantitative comparison of the area under different fluorescence phases, e.g., OPS and SMT of ChlF transients, for evaluating the parameters of ChlF decay from the peak P (F_P) to the semi steady-state S, e.g., t_{50} (the time to reach 50% of the fluorescence intensity from the peak P to the S level) and the associated rate constant (k), and for calculating the applicable tests (t test, one-way ANOVA, two-way ANOVA) to evaluate statistical significance of differences between the parameters. For evaluating the areas under different phases (OPS, $S_1M_1T_1$, and $S_2M_2T_2$), F_O was set as a baseline for each curve; lower and upper limits of points in the x-axis were manually controlled for obtaining precise and accurate integration of the area under each peak. The CO_2 induction curve was fitted using distance-weighted least-squares function, and then the IS_{60} and IT_{50} were calculated.

Results

Cold acclimation induced changes in ChlF transients of detached *Arabidopsis* leaves

ChlF transients of detached leaves of NAC and AC plants, measured at ~ 22 °C, upon illumination with low (40 µmol

photons m^{-2} s^{-1}) actinic orange (620 nm) light are shown in Fig. 2 (solid lines) (here, and in all the following figures, we do not include the relaxation of $F''_m(t)$ in the ChlF transients for better presentation of the slow fluorescence phase). The curves of ChlF transients are expressed as F/F_m since F_m was almost invariable in the measured temperature range.

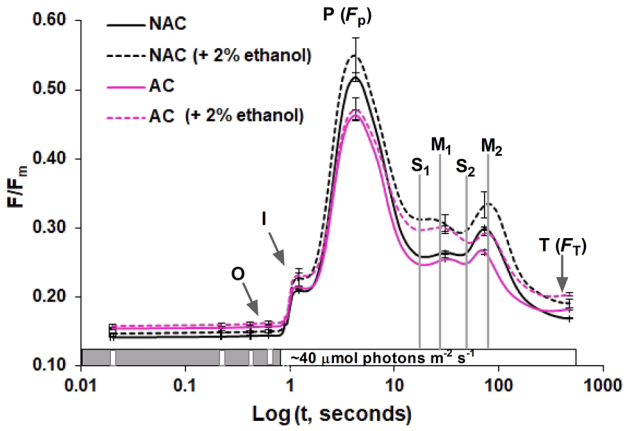

Fig. 2 Chlorophyll *a* fluorescence (ChlF) transients measured at 22 °C, and plotted as fluorescence intensity (F) at time (t), divided by maximum fluorescence intensity (F_m), against time, on log time scale. Samples were *Arabidopsis thaliana* accession C24 leaves, from both non-acclimated (NAC) and cold-acclimated (AC) plants; in addition, we show here data for both leaves when they were vacuum infiltrated with distilled water plus 2% ethanol. ChlF transients were measured as described in the legend of Fig. 1, but plotted as F/F_m, and on a logarithmic time scale, which allows for better visualization of the slow SMT phase (S is for semi steady-state; M for maxima; and T for terminal steady-state) (cf. Fig. 1 in Papageorgiou and Govindjee (2011)). Since there are two slow fluorescence waves, the S and M levels are labeled as S_1 & S_2 for the semi steady-state, and M_1 & M_2 for the maxima; the vertical lines are for the curve of NAC. See the legend of Fig. 1 for other details. For these experiments, $n=4$ or 8; standard errors (SE) are shown at several selected points on the curve

ChlF transients of both NAC and AC leaves show a rise in fluorescence intensity from the O (F_O) level to the peak P (F_P) followed by a slow decline that includes two fluorescence waves with maxima M_1 (NAC ~ 33.3 ± 0.4 s; AC ~ 31.2 ± 1.0 s) and M_2 (NAC ~ 72.6 s; AC ~ 66.7 ± 0.8 s) (Table 1), both being much lower than F_P (Fig. 2). The time to reach the P and the M_1 levels decreased with increasing actinic irradiance, from 80 to 160 µmol photons m^{-2} s^{-1}, while the time to reach the M_2 level increased. Fluorescence intensity at M_2 showed a stronger decrease at 160 µmol photons m^{-2} s^{-1} as compared to that at 80 µmol photons m^{-2} s^{-1} (see Supplementary Figs. S2A, S3A, and Table S1). Further, at ~ 300 µmol photons m^{-2} s^{-1}, both M_1 and M_2 were absent (see Supplementary Figs. S2B, S3B, and Table S1). A comparison of ChlF curves (Fig. 2) and the calculated parameters (Table 1) of NAC and AC leaves showed that cold acclimation significantly increased F_O ($p<0.01$) as well as the terminal steady-state fluorescence F_T ($p<0.01$), but decreased the F_P ($p<0.01$) and the M_2 ($p<0.05$) levels. Cold acclimation, when measured at 22 °C, did not show any effect on F_v/F_m (and, thus, Φ_{PSII}), but it significantly decreased the R_{FD} value (Table 1). Quantitative comparison of changes in ChlF transients from the peak P (F_P) to the semi steady-state S confirmed that two weeks of cold acclimation (AC) significantly increased k^{-1} and t_{50} by ~ 20%, ~ 4%, respectively, and decreased the value of $(F_P - F_S)/F_S$, by ~ 13%, as compared to their NAC counterparts (see Table 2).

Low temperature induced changes in ChlF transients in NAC and AC leaves

There was no significant difference in F_v/F_m between NAC and AC leaves during low-temperature treatment from 22 °C to − 1.5 °C; however, cooling down from 22 °C and 10 °C,

Table 1 The basic chlorophyll fluorescence parameters from detached leaves of non-acclimated (NAC) and cold-acclimated (AC) *Arabidopsis thaliana* accession C24

ChlF parameters	NAC	AC	NAC (+ethanol)	AC (+ethanol)
t_{Fp} (s)	3.4 ± 0	3.4 ± 0	3.4 ± 0	3.6 ± 0.3
t_{M1} (s)	33.3 ± 0.4	31.2 ± 1.0 (*)	23.2 ± 0	27.2 ± 2.5
t_{M2}(s)	72.6 ± 0.8	66.7 ± 0.8 (**)	79.2 ± 8.8	73.2 ± 7.0
F_o	0.141 ± 0.001	0.154 ± 0.002 (**)	0.147 ± 0.001	0.158 ± 0.001 (**)
F_p	0.52 ± 0.01	0.46 ± 0.01 (**)	0.55 ± 0.03	0.47 ± 0.01 (*)
F_{M1}	0.286 ± 0.003	0.267 ± 0.003 (***)	0.329 ± 0.006	0.289 ± 0.018
F_{M2}	0.312 ± 0.001	0.280 ± 0.002 (***)	0.347 ± 0.005	0.286 ± 0.018 (*)
F_T	0.168 ± 0.001	0.182 ± 0.002 (*)	0.191 ± 0.006	0.204 ± 0.002 (*)
F_v/F_m	0.853 ± 0.003	0.842 ± 0.002	0.849 ± 0.002	0.837 ± 0.007
Φ_{PSII}	0.790 ± 0.001	0.787 ± 0.004	0.766 ± 0.021	0.780 ± 0.019
R_{FD}	2.08 ± 0.04	1.58 ± 0.03 (***)	1.88 ± 0.06	1.33 ± 0.09 (***)

Mean ± SE ($n=4/8$ for AC/NAC). Asterisks (*) in the column of AC samples denote statistical significance of the data with respect to their NAC counterparts (*$p<0.05$, **$p<0.01$, ***$p<0.001$). See list of abbreviations for the definition of the parameters used here

Table 2 The effect of low temperature on several parameters: maximum quantum yield of PSII photochemistry (F_v/F_m), rate constant (k^{-1}), time to reach 50% from peak P to S (t_{50}), and the ratio $(F_P - F_S)/F_S$ for NAC and AC plant leaf samples

Temperature (°C)		F_v/F_m		k^{-1} (s)		t_{50} (s)		$(F_P - F_S)/F_S$	
		NAC	AC	NAC	AC	NAC	AC	NAC	AC
Control	22	0.853 ± 0.003	0.842 ± 0.002	14.3 ± 0.3	17.2 ± 0.4 (***)	7.23 ± 0.12	7.51 ± 0.07 (*)	1.01 ± 0.02	0.88 ± 0.03 (**)
+ 2%ethanol	22	0.849 ± 0.002	0.837 ± 0.007	16.6 ± 0.6	21.9 ± 3.9	6.91 ± 0.04	7.63 ± 0.41	0.76 ± 0.01	0.62 ± 0.05 (*)
	10	0.855 ± 0.002	0.845 ± 0.011	38.1 ± 7.6	30.8 ± 6.7	10.05 ± 0.87	8.81 ± 1.83	0.45 ± 0.05	0.59 ± 0.11
	4	0.841 ± 0.006	0.842 ± 0.010	–	54.6 ± 5.7	6.44 ± 0.47	9.57 ± 0.86 (*)	0.08 ± 0.01	0.35 ± 0.10
	0	0.837 ± 0.009	0.839 ± 0.010	–	–	7.12 ± 0.12	9.91 ± 3.15	0.10 ± 0.07	0.34 ± 0.10
	− 1.5	0.827 ± 0.009	0.830 ± 0.012	–	–	10.32 ± 0.21	7.28 ± 0.46 (*)	0.08 ± 0.01	0.24 ± 0.13

Mean ± SE [$n = 3/5$ (for control, 7/8) AC/NAC]. Asterisks (*) in the column of AC samples denote statistical significance of the data with respect to their NAC counterparts (*$p < 0.05$, **$p < 0.01$, ***$p < 0.001$)

respectively, to − 1.5 °C had a significant effect on F_v/F_m in NAC leaves, but not in AC leaves (Table 2). ChlF transients of the leaves of the control NAC and AC plants, recorded at selected temperatures, during slow cooling from 22 °C to − 1.5 °C, showed temperature-dependent changes in the OPS phase as well as in the SMT phase of the ChlF transients (see panels A and B in Fig. 3). Cooling of NAC leaves to 10 °C slightly increased F_P (~ 4%), but further cooling to 4 °C, 0 °C, and − 1.5 °C significantly reduced its value by ~ 42%, 37%, and 33%, as compared to that measured at 22 °C (Fig. 3A). We do not yet understand the reasons for this change. On the other hand, in AC leaves cooling to 10 °C and 4 °C, respectively, increased the level of F_P by 19% and 28%, while further cooling to 0 °C and − 1.5 °C brought back its value close to what was observed at 22 °C (Fig. 3B). For quantitative evaluation of effects of low temperature on ChlF transients, we compared the changes in the areas under the OPS (with peak F_P) and the SMT (with peaks M_1 and M_2) phases during cooling (see panels C and D of Fig. 3). At 22 °C, the area of the fast OPS phase was smaller (by ~ 8.3% in NAC and by ~ 16.6% in AC leaves) as compared to that under the SMT phase (with ~ 0.6% for M_1 and ~ 90.1% for M_2 in NAC; and ~ 2.3% for M_1 and ~ 81.1% for M_2 in AC). Further cooling below 10 °C led to a decrease of the OP phase, followed by an increase of the SMT phase, where the area under M_1 predominated over that under M_2 (see Fig. 3C, D).

The time to reach F_P (~ 3.4 s) was essentially unaffected by low-temperature treatment, except in the NAC leaves when cooled to − 1.5 °C; we found that, at this temperature, the position of F_P was delayed by ~ 6 s as compared to that measured at 22 °C (Table 3). At 10 °C, 4 °C, 0 °C, and − 1.5 °C, the intensity of the peak M_1 in the NAC samples increased by ~ 26%, 33%, 47%, 57%, as compared to that measured at 22 °C (Fig. 3A). However, in AC samples, cooling to the same temperatures increased the intensity of M_1 by ~ 19%, 68%, 75%, and 81%, respectively (Fig. 3B). The linear cooling caused high fluctuations in the position of peak M_1, but it significantly increased the time to reach M_1 in both the NAC and the AC leaves, as compared to that measured at 22 °C (Table 3; Fig. 3A, B). The position of M_2 in NAC leaves showed shifts of 124 s, 128 s, 297 s, and 235 s with reduced intensity, when cooled to 10 °C, 4 °C, 0 °C, and − 1.5 °C, respectively (Table 3; Fig. 3A). For AC samples, the position of M_2 was shifted by 44 s and 160 s when cooled to 10 °C and 4 °C, respectively, and its intensity was also reduced. However, further cooling abolished the M_2 peak (Table 3; Fig. 3A). In addition, a continuous increase in F_T during the low-temperature treatment was observed for both the NAC and the AC leaves (Fig. 3A, B). We note that cooling induced an increase in the intensity of F_P at 10 °C in the NAC, and at 10 °C and 4 °C in the AC leaves. This was accompanied by an increase in k^{-1} or t_{50}, but this was transient, peaking at a lower temperature in AC than in the NAC leaves (Table 2). The decrease in the fluorescence intensity from the P to the S level, as represented by the "quenching" ratio $(F_P - F_S)/F_S$, was shown by Briantais et al. (1979) to be linearly related to the transmembrane proton difference. In our experiments, low-temperature treatments decreased the P–S quenching ratio $(F_P - F_S)/F_S$, and at − 1.5 °C, this ratio decreased by ~ 92% and ~ 73%, respectively, in NAC and AC leaves, as compared to its value at 22 °C (Table 2). Further, we found that the correlation between the P–S quenching ratio and temperature was stronger in NAC than in AC leaves (R^2 of 0.94 vs. 0.82). Comparatively higher value of quenching ratio, at − 1.5 °C, and lower R^2 between this quenching ratio and temperature for AC leaves may indicate that cold-acclimated plants have a higher capacity to energize thylakoids by pumping comparatively more protons (H^+s) into the lumen; in other words, they seem to be able to induce a steeper proton concentration difference (ΔpH) across the thylakoid membrane, which may favor cyclic electron flow through PSI for adjusting the rate of ATP production, according to the metabolic needs of the sample (see, e.g., Shikanai 2007).

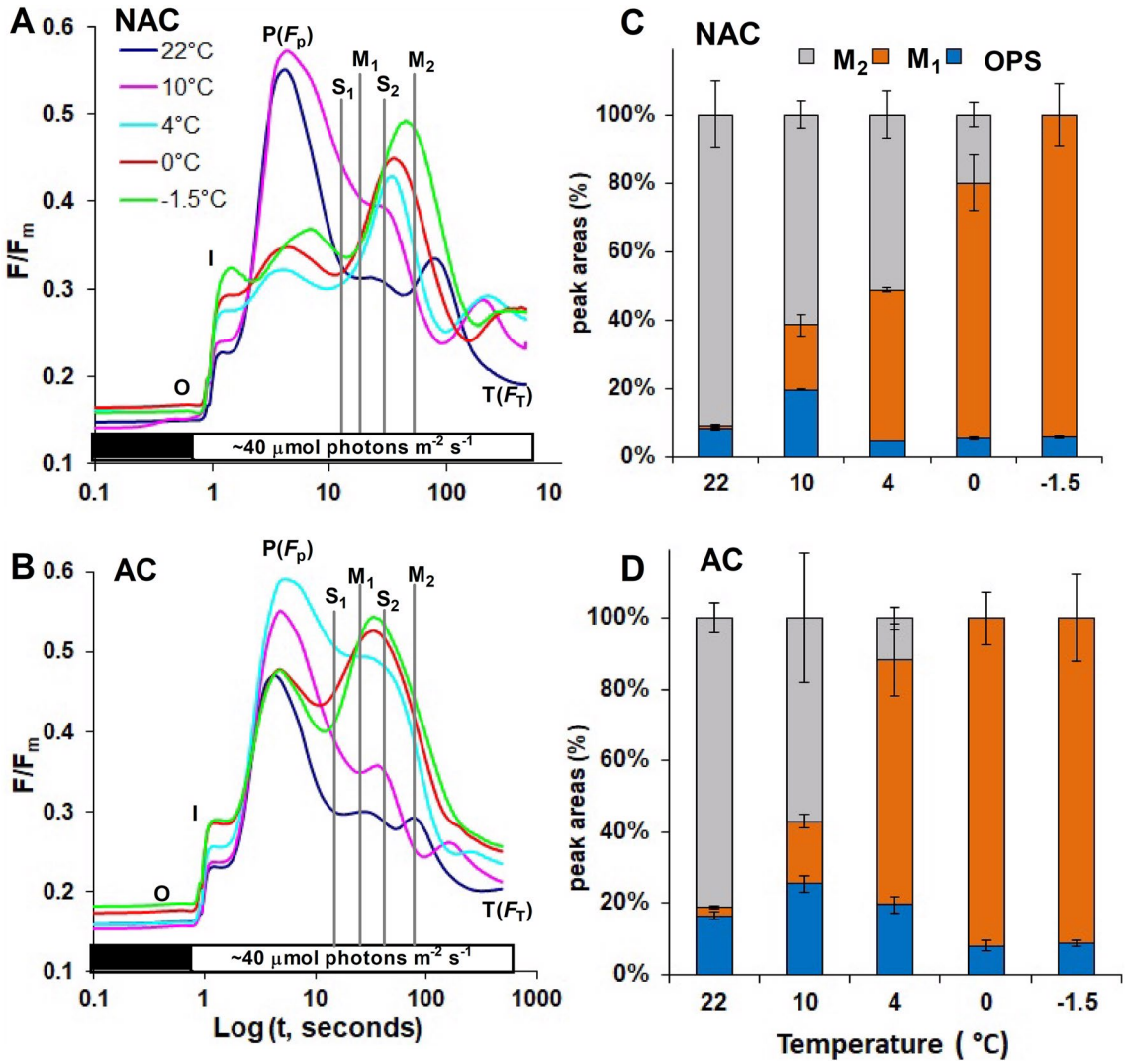

Fig. 3 Chlorophyll *a* fluorescence transients of leaves of NAC (**A**) and AC (**B**) *Arabidopsis thaliana* accession C24 at selected temperatures inside the freezer; samples were cooled at the rate of 2 °C h^{-1}. Corresponding cooling induced modifications of areas under the OPS [with peak P (F_P)] phase and the SMT phase (with peaks M_1 and M_2) are shown in panels **C** (NAC) and **D** (AC). In the panels **A** and **B**, the vertical lines at semi steady-states S_1 & S_2, and at maxima M_1 & M_2, are for the curves measured at 22 °C. Other experimental conditions are as described in the legends of Figs. 1 and 2

Table 3 The effect of low temperature on time in seconds to reach P (t_{F_P}), M_1 (t_{M1}) and M_2 (t_{M2}), for NAC and AC plant leaves. Mean ± SE (n = 4 for AC and 3 for NAC)

Temperature (°C)		t_{F_P} (s)		t_{M1} (s)		t_{M2} (s)	
		NAC	AC	NAC	AC	NAC	AC
+2% ethanol	22	3.4 ± 0	3.6 ± 0.3	23.2 ± 0	27.2 ± 2.5	79.2 ± 8.8	73.2 ± 7
	10	4.2 ± 0	3.6 ± 0.3	28.2 ± 1.2	35.2 ± 1.9 (*)	203.2 ± 16.8	117.9 ± 9.8 (**)
	4	3.9 ± 0	4.7 ± 0.6	29.5 ± 2.9	36.2 ± 6	207.2 ± 13.1	233.4 ± 23.9
	0	3.3 ± 0.8	4.5 ± 0.6	35.2 ± 5	33.2 ± 3.1	376.7 ± 40.5	--
	−1.5	9.2 ± 3.0	3.8 ± 0.2 (*)	37.1 ± 7	33.2 ± 1	315 ± 46	--

For control samples, detached leaves were used after vacuum infiltration in distilled water containing 2% of ethanol. Asterisks (*) in the column of AC samples denote statistical significance of the data with respect to their NAC counterparts (* $p < 0.05$, ** $p < 0.01$, *** $p < 0.001$)

Low temperature induced changes in the quantum yield of photochemical and regulated and non-regulated non-photochemical quenching

Low temperatures induced changes in the quantum yield of PSII photochemistry (Φ_{PSII}), of regulated NPQ (Φ_{NPQ}), and of the sum of quantum yields of fluorescence and basal constitutive thermal dissipation ($\Phi_{f,d}$), as evaluated according to the energy partitioning approach (see Hendrickson et al. 2004). Our data, recorded for NAC as well as AC leaves, are shown in Fig. 4. Contribution of the regulatory quantum yield of NPQ, Φ_{NPQ}, is very small (~4%) as compared to $\Phi_{f,d}$ (~18%) and Φ_{PSII} (~78%) for both NAC and AC at 22 °C. Both the Φ_{NPQ} and the Φ_{PSII} decreased by 2% with cooling until 4 °C; however, they had almost similar values for NAC and AC leaves (Fig. 4). Reductions in the Φ_{NPQ} and Φ_{PSII}, while cooling down to at 4 °C, were compensated by similar increases in $\Phi_{f,d}$. However, further cooling to 0 °C and − 1.5 °C led to an increase in the contribution of Φ_{NPQ} to 10% and 20% in NAC, and to 7% and 15% in AC leaves, and this increase in the Φ_{NPQ} was compensated by a decrease in the Φ_{PSII}. Significantly higher Φ_{NPQ} and lower Φ_{PSII} were observed in leaves of NAC (Fig. 4A) as compared to those from AC (Fig. 4B) plants at both 0 °C and − 1.5 °C.

In order to further investigate non-photochemical processes being affected by low temperatures under the prevailing actinic irradiance, we evaluated components of quantum yield of NPQ, Φ_{NPQ}: (1) a fast reversible energy-dependent quenching caused by ΔpH (Φ_{qE}), (2) a slow reversible phosphorylation of light-harvesting complexes of PSII that stimulates state-transition quenching (Φ_{qT}; *State I* to *State II*), and (3) the slowest of all, the photoinhibitory quenching (Φ_{qI}), in both the NAC and the AC leaves at selected temperatures (Fig. 5). Although Φ_{NPQ} declined during the initial cooling from 22 to 4 °C, we did not find any statistically significant

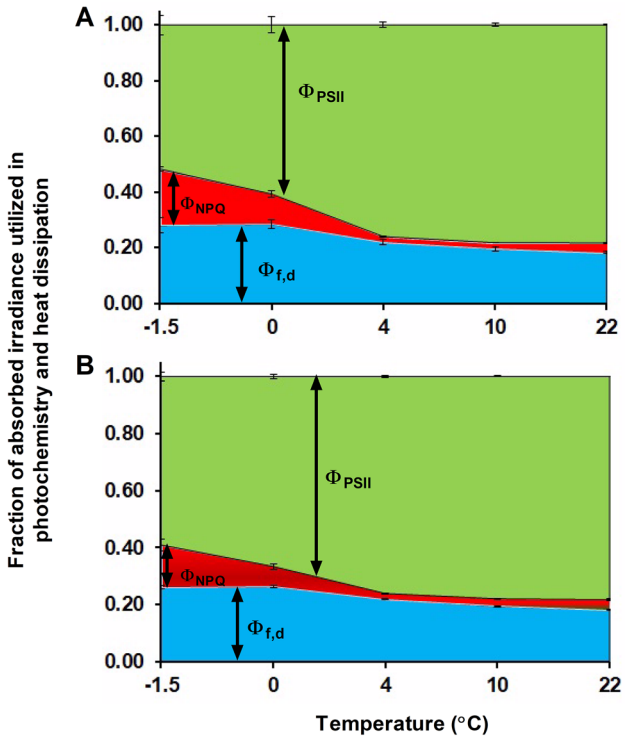

Fig. 4 Estimated quantum yields of PSII photochemistry (Φ_{PSII}), of regulated non-photochemical quenching (Φ_{NPQ}) and of non-regulated basal constitutive thermal dissipation and fluorescence ($\Phi_{f,d}$) for NAC (**A**) and AC (**B**) *Arabidopsis thaliana* accession C24, measured at selected temperatures during cooling. We have used the method given by Hendrickson et al. (2004) for estimating $\Phi_{PSII} = (F'_m - F_T)/F'_m$; $\Phi_{NPQ} = F_T/F'_m - F_T/F_m$; and $\Phi_{f,d} = F_T/F_m$. For details, see Material and Methods and Supplementary Fig. S1. Standard errors (± SE) are shown ($n = 3$ or 4)

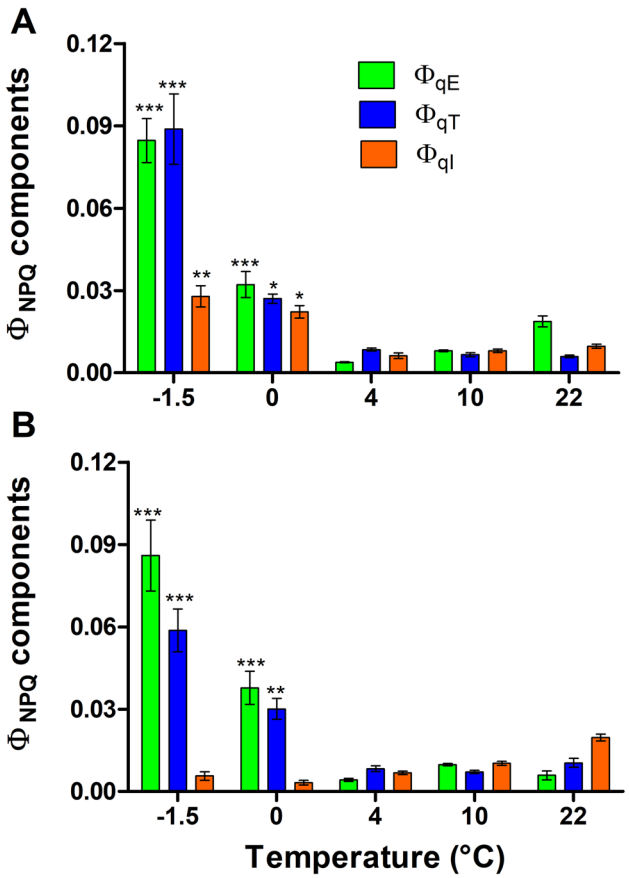

Fig. 5 Components of quantum yield of regulated non-photochemical quenching (Φ_{NPQ}) measured from the detached leaves of NAC (**A**) and AC (**B**) *Arabidopsis thaliana* accession C24. Φ_{qE} is the quantum yield for high-energy quenching, Φ_{qT} is the quantum yield of state change (*State I* to *State II*), and Φ_{qI} is the quantum yield of photoinhibition. For measuring components of Φ_{NPQ}, ChlF transients of the corresponding leaves were measured for 15 min under actinic light, followed by the measurement of relaxation of variable fluorescence at different time intervals for another 20 min in the dark, and their values were calculated as described by Guadagno et al. (2010). For further details, see Material and Methods and Supplementary Fig. S1. Standard errors (± SE) are for $n = 3$ or 4

difference between the different components of Φ_{NPQ} in both NAC and AC leaves (Fig. 5). A two-way ANOVA confirmed a significant increase in Φ_{qE}, Φ_{qT}, as well as in Φ_{qI}, in NAC leaves (Fig. 5A), whereas in the AC leaves, the increase was significant only for Φ_{qE} and Φ_{qT} and the value of Φ_{qI} remained similar to that at the higher temperatures (Fig. 5B).

Low temperature induced changes in fluorescence spectra at room temperature

We observed that low temperatures induced a larger increase in the far-red fluorescence band (F735, due to both PSII and PSI; cf. Agati et al. 2000; Franck et al. 2002; Lamb et al. 2018) than in the red fluorescence band (F683, mostly due to PSII), and this rise was most prominent at − 1.5 °C in NAC (Fig. 6A). However, in AC (Fig. 6B) leaves, it was prominent not only at − 1.5 °C but also at 4 °C and 0 °C. This caused a decrease in F683/F735 by ~ 7% for NAC at − 1.5 °C and ~ 8%, 19%, and 23% for AC at 4 °C, 0 °C, and − 1.5 °C, respectively, as compared to the values at 10 °C, which were 3.02 ± 0.08 (for NAC) and 3.40 ± 0.07 (for AC). Such a change could mean that low temperatures promoted *State I* to *State II* change, but in view of the complexities involved in deciphering PSI and PSII fluorescence at room temperature (see above, and Govindjee and Yang 1966; Franck et al. 2002), this conclusion cannot be made. Thus, we measured emission spectra at 77 K (see below).

Low temperature induced changes in fluorescence spectra at 77 K

To obtain information on low-temperature-induced state transitions (Fork and Satoh 1986; Kaňa et al. 2012), affected possibly by "migration" of LHCs between PSII and PSI, we measured 77 K ChlF spectra of leaf discs from NAC and AC plants. The samples were either directly taken from their adaptive growth temperatures or after low-temperature treatment at − 1.5 °C (Fig. 6C). The F695 band (at 77 K) is known to originate from Chls in CP47 and the F683 from Chls in both CP43 and CP47 (see, e.g., Andrizhiyevskaya et al. 2005); in addition, data of Chen et al. (2015) suggest that F683 may also include a contribution of RC Chls. Further, it is known that the F735 band (at 77 K) originates mostly from Chl *a* in PSI (see reviews in Govindjee et al. 1986; and Papageorgiou and Govindjee 2004). Our results show that cold acclimation led to a reduction in the intensity of the F735 band by ~ 22% in AC as compared to that in NAC plants (Fig. 6C); F683/F735 increased from 0.226 ± 0.009 in NAC leaves to 0.290 ± 0.018 in AC leaves (~ 28%, $p < 0.01$), indicating that cold acclimation "shifts" LHCs towards PSII, a slightly larger *State II* to *State I* transition in AC plants. However, when treated at − 1.5 °C, this band of both NAC and AC leaf samples was broadened,

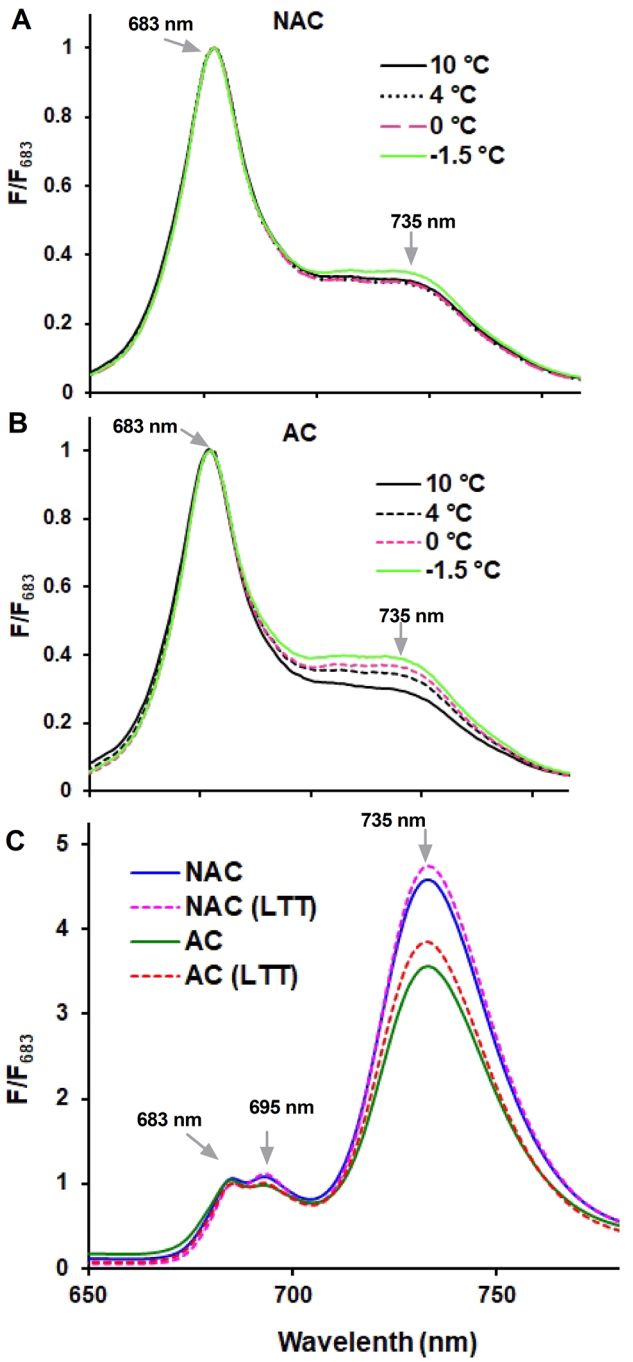

Fig. 6 Chlorophyll *a* fluorescence spectra of detached leaves (kept with their petioles under water) of the **A** NAC and **B** AC *Arabidopsis thaliana* accession C24 at several temperatures (ranging from 10 °C to − 1.5 °C), and **C** 77 K spectra for both NAC and AC leaf discs, with and without low-temperature treatment (LTT) at − 1.5 °C (slow cooling: 2 °C h^{-1}). The steady-state spectra presented in panels A and B were measured through fiber-optic cables by using 480 nm excitation light (obtained from a xenon lamp) of compact FluorMax 3 spectrofluorometer (Jobin Yvon). For measuring 77 K ChlF spectra, samples were placed inside liquid nitrogen, and spectra were recorded by a spectrofluorometer, described under Material and Methods; excitation was at 470 nm ($\Delta\lambda = 20$ nm). F_{683} stands for intensity of fluorescence at 683 nm. These spectra were normalized at 683 nm and data are averages of 3 or 5 leaves from different plants

but the ratio F683/F735 was significantly reduced by 13% ($p < 0.05$) only in leaves from the AC plants, indicating that − 1.5 °C causes *State I* to *State II* change, as implied by room temperature data (see above).

Effects of DCMU and methyl viologen (MV) on ChlF transients of NAC and AC leaves at room temperature

In order to investigate the impact of cold acclimation and low temperatures on specific photochemical processes, we measured ChlF transients of detached leaves treated with DCMU (that blocks electron flow between Q_A and the PQ pool, and thus, from PSII to PSI; see Holub et al. 2007) and MV (that accepts electrons from PSI; see Munday and Govindjee 1969). For both AC and NAC plant leaves, 20-s vacuum infiltration (at ~400 mbar) with 2% ethanol had negligible effects on the pattern of ChlF transients, including the SMT fluorescence phase (dotted lines in Fig. 2), and on several ChlF parameters, such as the maximum and effective quantum yield of PSII photochemistry (F_v/F_m reflecting Φ_{PSII}) and the time to reach F_P (t_{Fp}) (Table 1). Although vacuum infiltration did cause an increase in F_O and F_T, and a decrease in R_{FD}, in both NAC and AC samples, yet differences in these parameters between NAC and AC leaves were preserved (Table 1). Further, vacuum infiltration of detached leaves with 2% ethanol had insignificant effects on k^{-1} (t_{50}) and $(F_P - F_S)/F_S$ in AC plants; however, the same treatment significantly increased k^{-1} by 2.3 s (16%) and decreased $(F_P - F_S)/F_S$ to ~25% in NAC plants (Table 2).

To check if the vacuum-infiltrated chemicals indeed entered leaf discs, ChlF transients were measured at 22 °C. Clear and significant effects were observed in ChlF transients of leaves from both NAC (solid lines of Fig. 7) and AC (dotted lines see Fig. 7) plants. We conclude that higher concentrations of chemicals were needed in the leaves from NAC as compared to those from AC plants: (1) 200 µM of DCMU did not fully abolish the P to S decay of the ChlF transients in NAC leaves (blue solid line of Fig. 7), whereas 100 µM DCMU abolished both the fast P–S and slow SMT fluorescence phase in AC leaves (blue dotted line of Fig. 7); (2) increasing concentrations of MV gradually decreased the slow SMT phase, and 500 µM MV was enough to eliminate the SMT phase in NAC (solid magenta line of Fig. 7), whereas only 100 µM MV was needed to do the same in AC samples (dotted magenta line of Fig. 7).

Low-temperature treatment modifies the slow SMT phase in DCMU and MV-infiltrated leaves

In order to investigate effects of low temperature on ChlF transients of leaves with fully abolished SMT phase (e.g., when infiltrated with DCMU or MV), we measured ChlF transients of AC leaves treated with 100 µM DCMU (Fig. 8A), as well as with 100 µM MV (Fig. 8B), during cooling from 22 °C down to − 1.5 °C. For a comparison of changes in the SMT fluorescence phase, we plotted the

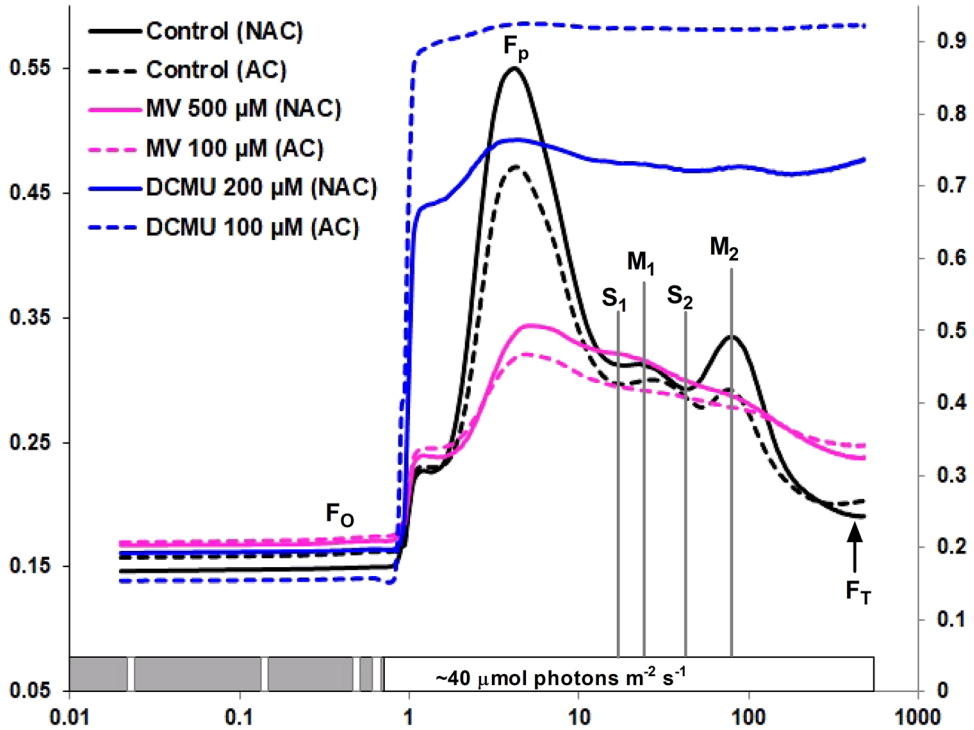

Fig. 7 Chlorophyll *a* fluorescence transients, measured at 22 °C, of NAC (solid lines) and AC (dotted lines) leaves of *Arabidopsis thaliana* accession C24 for the controls and those treated with 3-(3,4-dichlorophenyl)-1,1- dimethylurea (DCMU) or methyl viologen (MV); for details, see Material and Methods. The *y*-axis (on the right side) shows F/F_m data for DCMU-treated leaves, whereas that on the left is for controls and those treated with MV; further, the curves have been staggered to allow easier observation of differences between the different samples. Control samples were treated with distilled water containing 2% ethanol. The vertical lines at S_1 & S_2, and at M_1 & M_2, are for the curve indicated as control (NAC). Other experimental conditions are as described in the legends of Figs. 1 and 2

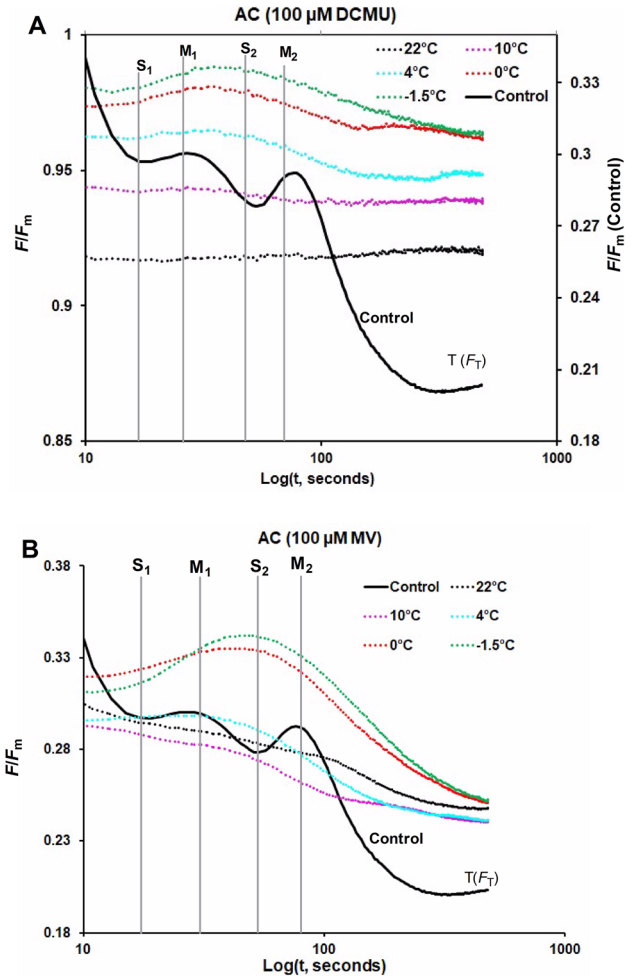

Fig. 8 Chlorophyll *a* fluorescence transients, measured at different temperatures during slow cooling (2 °C h^{-1}) of DCMU-treated (**A**) and MV-treated (**B**) (see Material and Methods for details) detached leaves of AC *Arabidopsis thaliana* accession C24. The y-axis (on the left) is F/F_m, and the y-axis (on the right) of the upper panel (**A**) is for ChlF transients of control leaves at room temperature (black line); these curves have been staggered to allow easier observation of differences between the different samples. The vertical lines, at semi steady-state S_1 & S_2 and at maxima M_1 & M_2, are for the curve indicated as control in both the panels. Control leaves were vacuum infiltrated in distilled water plus 2% ethanol. The ChlF transient was measured as described in the legends of Figs. 1 and 2; all data are plotted on a log time scale

data on a log scale starting at 10 s in Fig. 8. Corresponding data for NAC leaves treated with 200 µM DCMU and 500 µM MV are not shown here (however, see Supplementary Fig. S4). Our data show that in both DCMU- and MV-infiltrated leaves of NAC plants, the SMT phase was present at ~ 10 °C (Fig. S4), whereas in AC leaves, SMT fluorescence phase re-appeared only at ~ 4 °C (Fig. 8). In both DCMU- and MV-infiltrated leaves, SMT fluorescence phase was prominent both at 0 and − 1.5 °C (Fig. 8).

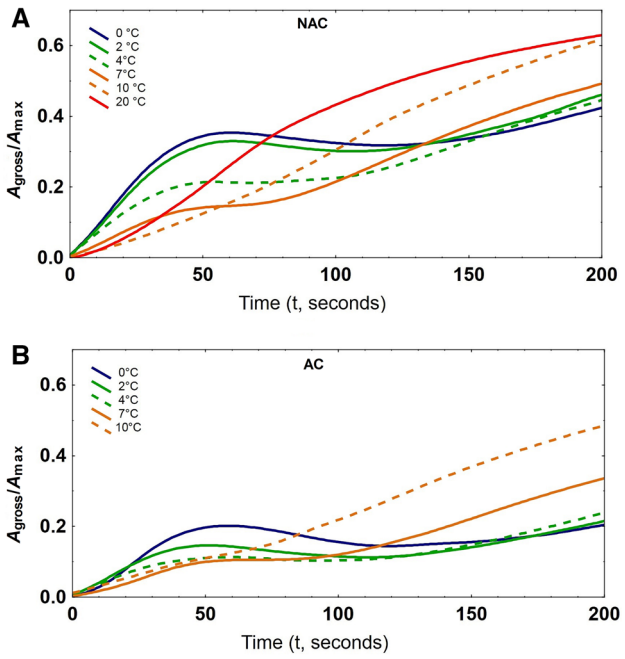

Fig. 9 Ratio of gross CO_2 assimilation rate (A_{gross})/maximum assimilation rate (A_{max}), measured at different temperatures on 45-min dark-adapted whole plants of NAC (panel **A**) and AC (panel **B**) *Arabidopsis thaliana* accession C24. Plants were exposed to 300 µmol photons m^{-2} s^{-1} (RGB light source). In this experiment, we observed different induction curves of CO_2 assimilation during the first 200 s. The measured CO_2 assimilation rate (A) was normalized with the rosette area for each plant and A_{gross} was estimated by adding respiration rates to net CO_2 assimilation rates. Curves are averages of three replicas for both AC and NAC plants that were further smoothened by distance-weighted least-squares function

Effects of cold acclimation and low-temperature treatment on whole plant CO_2 assimilation rate

For finding a relationship between the dynamics of the low-temperature-induced changes in ChlF transients and photosynthesis, we measured CO_2 assimilation rate (A) of NAC and AC plant rosettes at selected low temperatures during cooling down to 0 °C. A comparison of the ratio between the induction of light-induced gross CO_2 assimilation rate (A_{gross}) and the maximal CO_2 assimilation rate at saturating light (A_{max}) of NAC and AC plant rosettes, for the first 200 s after the light was switched on, is shown in Fig. 9. For both NAC and AC plant rosettes, the induction curves of A_{gross} were almost linear at 10 °C. However, there is an inflection with a peak at ~ 50 s in the induction curve from both AC and NAC plants at temperatures below 7 °C. Lowering the temperature broadened this peak and prolonged the position of its maximum by ~ 10 s at 0 °C (Fig. 9); note that the CO_2 assimilation in AC plant rosettes was measured only in the range of 10 °C to 0 °C. Surprisingly, for the AC plants, the initial photosynthetic induction was slower than that for the NAC plants (Fig. 9). Nevertheless, under saturating light, the

A_{gross} was significantly higher in the AC plants, as expected (Supplementary Fig. S5A). In both groups, however, A_{gross} declined with temperature, and at 0 °C the NAC and AC leaves had approximately the same A_{gross} (Supplementary Fig. S5A). Low temperature (e.g., 0 °C) significantly ($p < 0.01$) increased the time to reach 50% of the A_{max} (IT_{50}) in AC plants as compared to its value at 10 °C, whereas IT_{50} was almost constant below 7 °C in NAC plants. Further, at 7 °C and below, IT_{50} of AC plants was significantly higher than in the NAC plants (Supplementary Fig. S5B). For a better understanding of the low-temperature-induced peak during the initial induction of CO_2 uptake (Fig. 9), the induction of CO_2 assimilation rate at 60 s as a percentage of A_{gross} [IS_{60}(%)] is shown in Supplementary Fig. S5C. It is clear that this peak is much more pronounced in NAC than in AC plants, and its intensity is significantly higher below 7 °C, while for AC plants its rise is significantly lower for temperatures below 7 °C (Supplementary Fig. S5C).

Discussion

Effect of cold acclimation is reflected in chlorophyll fluorescence transients

Several parameters of ChlF transients are known to provide important insights into the molecular processes of photosynthesis in different photosynthetic organisms and under different biotic and abiotic stresses (Baker and Rosenqvist 2004; Baker 2008; Papageorgiou and Govindjee 2011; Gururani et al. 2015; Mishra et al. 2016a). The shape of the slow ChlF transients is affected by complex interactions within the photosynthetic machinery (this includes PSII, PSI, and associated LHCs, see Lazár 2015 for a review); ChlF transient is highly variable, and it has been used to obtain information on the qualitative effects of different experimental conditions on the photosynthetic processes (Strasser et al. 1995a, b; Govindjee 1995; Lazár 1999; Oxborough 2004; Kaňa and Govindjee 2016). Because of the observed large variations in the OPS and SMT fluorescence phases of ChlF transients, we have used specific quantitative features of ChlF transients, such as the rate constant (k) and the time to reach 50% of P–S quenching (t_{50}), as well as the areas underneath OPS and SMT phases, in order to understand the effects of low temperature, discovered in this work. These quantitative parameters proved to be highly valuable for the analysis of slow phase of ChlF transients (see the following sections).

We show here that although cold acclimation of C24 *Arabidopsis* did not change the pattern of ChlF transients (including the slow SMT phase) in NAC plants (Fig. 2), it significantly affected various parameters of these transients (Tables 1, 2). Variation in some of these parameters may be due to low-temperature-induced modification of the structural and functional properties of the chloroplasts, changed Chl content, and changes in rates of CO_2 assimilation, carbon metabolism, and other photosynthetic activities (cf. Telfer et al. 1976; Martindale and Leegood 1997; Strand et al. 1999). However, an increase in the minimal fluorescence (F_O) of cold-acclimated leaves (Fig. 2) points to modulation in light-harvesting chlorophyll antenna size of one or both photosystems and their activities, whereas an increase in the time needed for the P-to-S decline in cold-acclimated leaves (Fig. 2), as shown by an increase in k^{-1} (or t_{50}) (Table 2), may indicate structural changes or changes in acidification of the thylakoid lumen (Briantais et al. 1980; Walters et al. 1996) and/or in events related to carbon fixation (Walker 1981; Seaton and Walker 1990; Savitch et al. 1997). Further, comparatively higher terminal steady-state fluorescence (F_T), at 22 °C, in AC leaves under identical exposure of actinic irradiance, may indicate a shift of energy distribution in different pathways in order to have efficient photochemical and carbon fixation reactions of photosynthesis at low temperatures.

Low-temperature treatment largely affects the slow phase of ChlF transient and the CO_2 assimilation induction curve

We show here that lowering of temperature has a marked effect on ChlF transients in the leaves of both the NAC and the AC plants (Fig. 3A, B), and these changes are reflected in the quantitative parameters, e.g., areas underneath the OPS and the SMT fluorescence phases (Fig. 3C, D), peak positions, and the values of k, t_{50}, and $(F_P - F_S)/F_S$ (Tables 2, 3). The O–P rise is mainly due to the closure of PSII reaction centers with the reduction of primary electron acceptor Q_A, as well as electron acceptors beyond PSI (in other words, it reflects the reduction of the entire electron transport chain); in the presence of saturating light, Q_A is fully reduced to Q_A^-, and F_P attains the value of F_m (Govindjee 1995; Baker 2008; Stirbet and Govindjee 2011, 2012). Cold acclimation essentially changes the redox state of photosynthetic electron transport components; in part, this is due to Q_A being kept in the oxidized state (see Huner et al. 1998) and by changing the redox potential not only of Q_A, but also of Q_B (Sane et al. 2003; cf. Ensminger et al. 2006; Khanal et al. 2017). Any change in the ratio of Q_A to Q_A^-, obviously, changes the F_P level, when measured under identical light (here, measured at actinic irradiance of ~40 µmol photons m^{-2} s^{-1}).

ChlF transients beyond F_P are much more complex than the fast O–P rise (see, e.g., Stirbet and Govindjee 2016; Bernát et al. 2018) because of several processes, e.g., both photochemical and non-photochemical quenching, due to changes in the acidification of the thylakoid lumen, ATP synthesis, and the activation of the Calvin–Benson cycle. All of these affect ChlF, especially beyond F_P, and this is

reflected in changes in the parameter t_{50} (k^{-1}). Further, the corresponding areas underneath OPS would also be modulated. In addition to that, an indirect effect on the O–P curve must be considered. It has been demonstrated that the area above O–P reflects the size of the PSII acceptor pool, i.e., plastoquinone, and the oxidized carriers between PSII and the Calvin–Benson cycle, i.e., the acceptors of PSI (see, e.g., Joliot and Joliot 2002; Tóth et al. 2007). Given that low temperature slows down the Calvin–Benson cycle, a feedback that affects the O–P curve must also be expected.

In the ChlF transients from leaves of NAC and AC plants (Fig. 3A, B), the area under the M_1 peak increased with decreasing temperature, and this effect was much more pronounced in AC than in the NAC leaves (Fig. 3C, D). The time to reach M_1 (see Table 3) was about 10–25 s ahead of the peak in the CO_2 assimilation curve (see Fig. 9), indicating a link between the decline in fluorescence following M_1 and the initiation of carbon fixation. This is supported by the observation that the low-temperature-induced shift in the position of M_1 (Fig. 3; Table 3) coincides with a shift in the peak of the CO_2 assimilation (Fig. 9). Considering that the decrease of CO_2 fixation following the peak in the CO_2 assimilation curve and its shift most likely reflect exhaustion of Calvin–Benson cycle intermediates, our results may be interpreted to indicate a transition from carboxylation limitation to ribulose-bisphosphate (RuBP) regeneration-limited photosynthesis at low temperatures (Hikosaka et al. 2006). Low temperature may favor RuBP-limited photosynthesis when there are limitations on either (i) the rate by which the bisphosphatases, in the stroma, regenerate RuBP in the photosynthetic carbon reduction cycle, or (ii) the rate at which triose-phosphates are exported from the chloroplasts or metabolized to release inorganic phosphate (Pi) for use in subsequent photophosphorylation (Allen and Ort 2001). However, a direct effect of the electron transport processes on RuBP regeneration cannot be excluded. The time to reach 50% of A_{max} (IT_{50}) was much longer in AC, than in NAC, leaves (Supplementary Fig. S5B), which may indicate that enzymatic reactions of the Calvin–Benson cycle may take longer time for activation. Five of the enzymes of the Calvin–Benson cycle (Fructose-bisphosphatase, Sedoheptulose-bisphosphatase, Phosphoribulokinase, Glyceraldehyde 3-phosphate dehydrogenase, and Ribulose-1,5-bisphosphate carboxylase/oxygenase (Rubisco) via Rubisco activase) are known to be redox regulated via the thioredoxin-system (Buchanan 1991). Zhang and Scheller (2004) have shown that low temperature causes a persistent reduction in PSI activity, expressed as the rate of NADPH production, which is coupled to a reduced proportion of photo-oxidizable P700. Reduced photo-oxidation of P700 would affect the reduction of ferredoxin pool, and thus the activation of Calvin–Benson cycle enzymes might be affected. This may mean that increased F_P and F_T along with broadening of the OPS and $S_1M_1T_1$ fluorescence phases at suboptimal temperatures (at 10 °C for NAC, 10 °C and 4 °C for AC) may be induced by a slowdown in the electron transport chain, and that there exists a correspondence between further rise of the SMT (specifically with peak M_1) fluorescence phase (Fig. 3A, B) and the peak in the CO_2 assimilation curve (Fig. 9A, B). The latter seems to be due to limitations of photosynthesis by both the substrates of the Calvin–Benson cycle and/or RuBP regeneration (see Furbank and Walker 1986). Thus, ChlF transients can indeed be used to interpret changes in low-temperature-induced "light reactions" as well as the "carbon reactions" of photosynthesis.

Cold-acclimated plants have better modulation of quantum yield of regulated NPQ via state transition and photoinhibition at low temperatures

We have observed a significant decrease in F_v/F_m (at − 1.5 °C) and in F_P (at 4 °C and − 1.5 °C) in NAC, but not in AC, leaves (Fig. 3A, B; Table 2). This corresponds to a higher degree of quantum yield of photoinhibition, Φ_{qI}, in NAC leaves (Fig. 5A). Further, this may indicate a vulnerability of RCs of PSII in NAC leaves that may have resulted because of a block of the D1-repair cycle at low temperatures (Mohanty et al. 2007). Photoinhibition has been shown to be directly proportional to increasing light intensity (Tyystjärvi and Aro 1996), but its underlying mechanisms are complex and still not fully understood (Allakhverdiev et al. 2005, 2007; Tyystjärvi 2013; Khanal et al. 2017). Sane et al. (2003) reported, in *Arabidopsis* accession Col-0, that cold acclimation predisposes photoinhibition by facilitating radical pair backward recombination reactions of $P680^+ Q_A^-$ that enhances the dissipation of excess light energy within the reaction center of PSII.

Temperatures below 4 °C were shown here to lead to an increase in the quantum yield of regulated NPQ, Φ_{NPQ}, and a dramatic reduction in Φ_{PSII} especially in the NAC leaves (Fig. 4). Comparatively lower Φ_{NPQ} in AC leaves than that in NAC, at low temperatures, may be due to higher enzyme activity in the Calvin–Benson cycle, which is reflected in higher A_{gross} that may further allow the plant to keep high photochemical quenching. A simultaneous increase in Φ_{NPQ} and decline in Φ_{PSII} is an indicator of an activation of alternative electron transport pathways, e.g., cyclic electron transport through PSI (Ort and Baker 2002). Analysis of the different components of Φ_{NPQ} suggests that state transition (qT; see, e.g., Allen 2003; Horton 2012) involved in the re-distribution of LHCs from the high fluorescent PSII to the low fluorescent PSI has a significant role at temperatures near or below the freezing point (Fig. 5). Our results on the fluorescence emission spectra, measured during low-temperature treatment (Fig. 6), confirm this hypothesis. A comparison of 77 K spectra, and of F685/F735 ratios,

for AC and NAC leaves, before and after low-temperature (− 1.5 °C) exposure, further suggests that re-distribution of LHCs in favor of PSI, i.e., *State I* to *State II* transition, may indeed serve as a regulatory mechanism to protect the photosystems, and that cold acclimation may stimulate this process (Fig. 6C). Yun et al. (1997) reported destacking of inter-grana lamellae, after only 3 s of exposure to 5 °C, in the chilling-sensitive African violet (*Saintpaulia ionantha*). This led to homogeneous distribution of proteins within the thylakoid membrane and resulted in "spillover" of excitation energy from PSII to PSI (Agati et al. 2000). It is unlikely that destacking of grana was the reason for the decreased F685/F735 ratio in accession C24, as observed in our work, since this would have been accompanied by a large decrease in ChlF (Yun et al. 1997), which was not observed in C24 *Arabidopsis* plants. This points out to us that state transition must play a key role in cold-acclimated leaves, and that this process prevents high excitation pressure and damage of PSII during low-temperature exposure.

Analysis of ChlF transients in the presence of different photosynthetic inhibitors

When chemicals (such as DCMU and MV) that modify or interfere with the electron transport process were applied to NAC and AC leaves, it appeared that AC leaves required lower concentrations to give the same effect (Fig. 7). This might be due to lower water content of AC leaves that may have led to a general increase in the concentration of the solutes (Cook et al. 2004). As already mentioned above, the SMT fluorescence phase displayed two maxima (M_1 and M_2, see Fig. 2) at 22 °C, and that these were eliminated when leaves were exposed to an elevated irradiance of 300 µmol photons m^{-2} s^{-1} (Supplementary Figs. S2 and S3), as well as after infiltration with DCMU (Fig. 8A) or with MV (Fig. 8B). Thus, the development of the SMT phase, at 22 °C, is a typical feature of ChlF transients, at low irradiance, in *Arabidopsis* accession C24 (cf. results of Papageorgiou and Govindjee 1968a, b on algae and cyanobacteria). Our finding that low temperature modifies SMT and causes its re-appearance in leaves after complete elimination with DCMU or MV is a new observation, but the latter is much more difficult to understand. DCMU works by displacing plastoquinone Q_B of PSII, thus inhibiting the photosynthetic electron transport beyond Q_A, and therefore it prevents quenching of ChlF transients beyond F_P. The used low actinic irradiance, in 100 µM DCMU-treated AC leaves, increased F_P to 92% of F_m and inhibited ChlF quenching beyond F_P, thus eliminating the SMT fluorescence phase. Lowering the temperature caused F_P to increase, but it also caused the re-appearance of the M_1 in the time range (of the experiment) as it appeared without DCMU (Table 3). We interpret this as a temperature effect on the remaining electron transport activity, which was slowed down at lower temperatures, most significantly at the time interval of 50–60 s, when we also observed a retardation of carbon assimilation reactions.

Methyl viologen efficiently catalyzes electron transfer to oxygen instead of ferredoxin, thus not only stimulating linear electron flow, but also suppressing cyclic electron flow at PSI (Munday and Govindjee 1969; Joliot and Joliot 2006). Considering that MV effectively competes with electron transport to ferredoxin as well as to cytochrome b_6f, re-occurrence of the peak M (Fig. 8B) in MV-treated leaves at low temperatures indicates a slowdown in the electron transfer reactions competing with MV, which in turn must mean that, at low temperature, cyclic electron transport significantly contributes to the quenching of ChlF. This has been interpreted as a means to increase ATP production at low temperatures (Joliot and Johonson 2011; Kramer and Evans 2011), but it could also act as a regulatory factor in offsetting the slow turnover of NADPH in the Calvin–Benson cycle at the lower temperatures. Therefore, the re-appearance of maxima M in the ChlF transients at low temperatures might reflect a strategy for regulating photosynthetic efficiency through combination of processes that may include state transition (*State II* to *State I* transition) and cyclic electron transport (Fig. 8).

Regulation of slow SMT fluorescence phase

The SMT fluorescence phase has been observed in cyanobacteria (Papageorgiou and Govindjee 1968a), green algae (Papageorgiou and Govindjee 1968b; Mohanty and Govindjee 1974), red algae (Mohanty et al. 1971), lichens (Mishra et al. 2015; Marečková and Barták 2016), as well as in higher plants (Bradburry and Baker 1984; Pandey and Gopal 2012). It is highly pronounced in phycobilisome (PBS)-containing cyanobacteria; here, in contrast to other organisms, the intensity of the fluorescence maxima M is much higher than that of the peak P, F_P (Kaňa et al. 2012). As is known in several systems (Yamagishi et al. 1978; Fork and Satoh 1986; Papageorgiou et al. 2007; Papageorgiou and Govindjee 2011), the SMT fluorescence phase has two waves in *Arabidopsis* accession C24. Yamagishi et al. (1978) suggested that protonation-induced structural changes in thylakoids may partially contribute to the formation of the SMT phase in isolated chloroplasts from a green alga *Bryopsis maxima*. Sivak et al. (1985a) compared the ChlF transients and light scattering at 535 nm, in spinach leaves, after 1 min and 4 min of dark intervals, and found simultaneous changes in scattering and the formation of the SMT phase, in 4-min, but not in 1-min, dark-adapted leaves. Sivak et al. (1985a) assumed that longer dark adaptation transiently energizes thylakoids that induce high scattering at 535 nm because of the development of transmembrane proton difference, and

consequently, the SMT phase was formed due to low consumption of ATP in low irradiance. Sivak et al. (1985b) further interpreted the dynamics of the SMT phase as an "indicator of protonation of thylakoids" and found that the proton motive force increases and decreases slightly in advance of the rise and the fall of the CO_2 assimilation rate. Further, Bradbury and Baker (1981, 1984) have suggested that both the redox state of the PSII electron acceptor as well as an interplay between photochemical and non-photochemical quenching play a major role during the P–T decline, and the S–M rise is predominantly caused by a decrease in photochemical quenching (qP) that implies a decrease in the linear electron flow. This would agree with our interpretation of an involvement of insufficient RuBP regeneration as one of the causes for SMT development. Kaňa et al. (2012) have suggested that induction of SMT phase is a safe way of dissipating excess light in *Synechococcus* that lacks certain NPQ mechanisms. They have demonstrated that state transition is the major phenomenon behind the S–M rise; the S–M rise is due to transition of lower fluorescence "*State II*" to a higher fluorescence "*State I*" since a mutant blocked in state change did not show the S–M rise. It is possible that the M–T decline could be, partly, due to the "*State I*" to "*State II*" transition in cyanobacteria (Papageorgiou and Govindjee 2011; Kaňa et al. 2012; Bernát et al. 2018). A similar conclusion for S–M rise has been made for the green alga *Chlamydomonas reinhardtii* (Kodru et al. 2015). Further, our results show the occurrence of SMT as well NPQ at low temperatures in both the NAC and the AC leaves of *Arabidopsis* natural accession C24. Our data clearly show that state transition plays an important role in *Arabidopsis*, and that it is activated already at 4 °C in NAC plants, whereas in AC plants, it is prominent only at a lower temperature, − 1.5 °C.

Conclusions

We have demonstrated that cold acclimation modulates photosynthetic activity of a cold-sensitive natural *Arabidopsis* accession C24 since cold acclimation improves not only the CO_2 assimilation rate at saturating light, but also the maximum quantum yield of PSII photochemistry and the regulatory non-photochemical quenching at ~ 0 °C. We have discovered that cold acclimation slows down quenching reactions during the fluorescence decline from the P to S level, and this may facilitate improved quenching ratio (an indicator of proton pumping capacity) at low temperatures. We speculate that improvement in both photochemical and carbon reactions of photosynthesis may have been due to a general increase in the activity of several Calvin–Benson cycle enzymes (e.g., Rubisco) and regulatory proteins (e.g., thioredoxin) that better facilitate the regulation of photosynthesis at low temperatures. Furthermore, the estimated changes in the quantum yield of regulatory NPQ suggest that cold-acclimated plants develop an ability to reduce photoinhibition. On the other hand, the slow SMT fluorescence phase ($S_1M_1S_2M_2T$), measured at 22 °C, seems to reflect constraints in "photochemical pathways" because it disappears when exposed to high irradiance or after application of DCMU (blocking electron transport) and MV (accelerating electron transport). The redox state of Q_A and inhibition in kinetics of redox reactions of photosynthetic electron transport (between PSII and PSI and beyond) are expected to increase F_P, F_T, and the area underneath the OPS fluorescence phase at suboptimal temperatures (10 °C for NAC; 10 °C and 4 °C for AC plants). However, low temperature-induced strong modulation of the SMT fluorescence phase (in AC and NAC leaves), and re-appearance of the SMT phase in DCMU and MV treated leaves that had no SMT fluorescence phase at 22 °C, indicates a contribution of cyclic electron flow through PSI. Low-temperature-induced re-distribution of LHCs from PSII towards PSI also supports the possibility of cyclic electron transport through PSI being involved in the formation of SMT fluorescence phase. Further, we suggest that both the initiation of state transition and cyclic electron transport stimulate SMT fluorescence phase, at low temperatures, in response to limitations in the Calvin–Benson cycle and/or RuBP regeneration. Thus, there must exist a dynamic regulation of photochemical and biochemical activities in response to low-temperature treatment in *Arabidopsis* leaves, and low-temperature-induced restrictions on biochemical reactions are not only reflected in CO_2 assimilation rates but also in ChlF transient measurements that are more sensitive, and easier to use; they provide much more information for the same phenomena. Further research involving *Arabidopsis* mutants will help in reaching a better understanding of cold acclimation-induced modifications in the photosynthetic machinery.

Acknowledgements This work was supported by the Ministry of Education, Youth and Sports of the Czech Republic within the National Sustainability Program I (NPU I), grant number LO1415. The infrastructure used within this research was supported by the project CzeCOS Proces (CZ.02.1.01/0.0/0.0/16_013/0001609). We thank Radek Kaňa (Institute of Microbiology, ASCR, Třeboň, CZ) for providing us the fluorometer used for measuring the 77 K spectra. Govindjee thanks the Schools of Integrative Biology and Molecular and Cell Biology of the University of Illinois at Urbana-Champaign for their support. We are grateful to George C. Papageorgiou for critical reading of an earlier draft of this paper, and for his valuable comments.

References

Agati G, Cerovic ZG, Moya I (2000) The effect of decreasing temperature up to chilling values on the in vivo F685/F735 chlorophyll fluorescence ratio in *Phaseolus vulgaris* and *Pisum*

sativum: the role of the photosystem I contribution to the 735 nm fluorescence band. Photochem Photobiol 72:75–84
Ahn TK, Avenson TJ, Peers G, Li Z, Dall'Osto L, Bassi R, Niyogi KK, Fleming GR (2009) Investigating energy partitioning during photosynthesis using an expanded quantum yield convention. Chem Phys 357:151–158
Allakhverdiev SI, Klimov VV, Carpentier R (1997) Evidence for the involvement of cyclic electron transport in the protection of photosystem II against photoinhibition: influence of a new phenolic compound. Biochemistry 36(14):4149–4154
Allakhverdiev SI, Nishiyama Y, Takahashi S, Miyairi S, Suzuki I, Murata N (2005) Systematic analysis of the relation of electron transport and ATP synthesis to the photodamage and repair of photosystem II in synechocystis. Plant Physiol 137:263–273
Allakhverdiev SI, Los DA, Mohanty P, Nishiyama Y, Murata N (2007) Glycinebetaine alleviates the inhibitory effect of moderate heat stress on the repair of photosystem II during photoinhibition. Biochim Biophys Acta 1767(12):1363–1371
Allen JF (2003) State transitions—a question of balance. Science 299:1530–1532
Allen DJ, Ort DR (2001) Impacts of chilling temperatures on photosynthesis in warm-climate plants. Trends Plant Sci 6:36–42
Andrizhiyevskaya EG, Chojnicka A, Bautista JA, Diner BA, van Grondelle R, Dekker JP (2005) Origin of the F685 and F695 fluorescence in Photosystem II. Photosynth Res 84:173–180
Aro EM, Hundal T, Carlberg I, Andersson B (1990) In vitro studies on light-induced inhibition of photosystem-II and DI-protein degradation at low-temperatures. Biochim Biophys Acta 1019:269–275
Asada K (1999) The water–water cycle in chloroplasts: scavenging of activeoxygens and dissipation of excess photons. Annu Rev Plant Physiol PlantMol Biol 50:601–639
Baker NR (2008) Chlorophyll fluorescence: a probe of photosynthesis in vivo. Annu Rev Plant Biol 59:89–113
Baker NR, Rosenqvist E (2004) Applications of chlorophyll fluorescence can improve crop production strategies: an examination of future possibilities. J Exp Bot 55:1607–1621
Bernacchi CJ, Portis AR, Nakano H, Caemmerer SV, Long SP (2002) Temperature response of mesophyll conductance. Implications for the determination of Rubisco enzyme kinetics and for limitations to photosynthesis in vivo. Plant Physiol 130(4):1992–1998
Bernát G, Steinbach G, Kaňa R, Govindjee, Misra AN, Prášil O (2018) On the origin of the slow M–T chlorophyll *a* fluorescence decline in cyanobacteria: interplay of short-term light-responses. Photosynth Res 136(2):183–198
Berry J, Björkman O (1980) Photosynthetic response and adaptation to temperature in higher plants. Annu Rev Plant Physol 31:491–543
Bradbury M, Baker NR (1981) Analysis of the slow phases of the in vivo chlorophyll fluorescence induction curve. Changes in the redox state of Photosystem II electron acceptors and fluorescence emission from Photosystem I and II. Biochim Biophys Acta 635:542–551
Bradbury M, Baker NR (1984) A quantitative determination of photochemical and non-photochemical quenching during the slow phase of the chlorophyll fluorescence induction curve of bean leaves. Biochim Biophys Acta 765:275–281
Briantais JM, Vernotte C, Picaud M, Krause GH (1979) A quantitative study of the slow decline of chlorophyll *a* fluorescence in isolated chloroplasts. Biochim Biophys Acta 548:128–138
Briantais JM, Vernotte C, Picaud M, Krause GH (1980) Chlorophyll fluorescence as a probe for the determination of the photoinduced proton gradient in isolated chloroplasts. Biochim Biophys Acta 591:198–202
Buchanan BB (1991) Regulation of CO_2 assimilation in oxygenic photosynthesis: the ferredoxin/thioredoxin system. Perspective on its discovery, present status, and future development. Arch Biochem Biophys 288(1):1–9
Cailly AL, Rizza F, Genty B, Harbinson J (1996) Fate of excitation at PSII in leaves, the non-photochemical side. Plant Physiol Biochem (Special Issue): 86 (abstract)
Catalá R, Medina J, Salinas J (2011) Integration of low temperature and light signaling during cold acclimation response in Arabidopsis. Proc Natl Acad Sci USA 108(39):16475–16480
Chazdon RL, Pearcy RW (1986) Photosynthetic response to light variation in rainforest species. II Carbon gain and photosynthetic efficiency during lightflecks. Oecologia 69:524–531
Chen J, Kell A, Acharya K, Kupitz C, Fromme P, Jankowiak R (2015) Critical assessment of the emission spectra of various photosystem II core complexes. Photosynth Res 124:253–265
Cook D, Fowler S, Fiehn O, Thomashow MF (2004) A prominent role for the CBF cold response pathway in configuring the low-temperature metabolome of Arabidopsis. Proc Natl Acad Sci USA 101:15243–15248
Crosatti C, Rizza F, Badeck FW, Mazzucotelli E, Cattivelli L (2013) Harden the chloroplast to protect the Plant. Physiol Plant 147:55–63
Demmig-Adams B, Adams WW (2000) Harvesting sunlight safely. Nature 403:371–374
Demmig-Adams B, Grab G, Adams III WW, Govindjee (eds) (2014) Non-photochemical quenching and energy dissipation in plants, algae and cyanobacteria. In: series: advances in photosynthesis and respiration, vol 40. Springer, Dordrecht
Ehlert B, Hincha DK (2008) Chlorophyll fluorescence imaging accurately quantifies freezing damage and cold acclimation responses in Arabidopsis leaves. Plant Methods 4:12
Endo T, Kawase D, Sato F (2005) Stromal over-reduction by high-light stress as measured by decreases in P700 oxidation by far-red light and its physiological relevance. Plant Cell Physiol 46(5):775–781
Ensminger I, Busch F, Huner NPA (2006) Photostasis and cold acclimation: sensing low temperature through photosynthesis. Physiol Plant 126:28–44
Fork DC, Satoh K (1986) The control by state transitions of the distribution of excitation energy in photosynthesis. Annu Rev Plant Physiol 37:335–361
Franck F, Juneau P, Popovic R (2002) Resolution of the photosystem I and photosystem II contributions to chlorophyll fluorescence of intact leaves at room temperature. Biochim Biophys Acta 1556:239–246
Franklin KA. Whitelam GC (2007) Light-quality regulation of freezing tolerance in *Arabidopsis thaliana*. Nat Genet 39:1410–1413
Furbank RT, Walker DA (1986) Chlorophyll *a* fluorescence as a quantitative probe of photosynthesis: Effects of Co_2 concentration during gas transients on chlorophyll fluorescence in spinach leaves. New Phytol 104:207–213
Genty B, Briantais JM, Baker NR (1989) The relationship between the quantum yield of photosynthetic electron transport and quenching of chlorophyll fluorescence. Biochim Biophys Acta 990:87–92
Goltsev VN, Kalaji HM, Paunov M, Bąba W, Horaczek T, Mojski J, Kociel H, Allakhverdieve SI (2016) Variable chlorophyll fluorescence and its use for assessing physiological condition of plant photosynthetic Apparatus. Russ J Plant Physiol 63(6):869–893
Govindjee (1995) Sixty three years since Kautsky—Chlorophyll a fluorescence. Aust J Plant Physiol 22(2):131–160
Govindjee, Spilotro P (2002) An *Arabidopsis thaliana* mutant, altered in the γ-sub-unit of ATP synthase, has a different pattern of intensity-dependent changes in non-photochemical quenching and kinetics of the P-to-S fluorescence decay. Funct Plant Biol 29:425–434
Govindjee, Yang L (1966) Structure of the red fluorescence band in chloroplasts. J Gen Physiol 49:763–780

Govindjee, Amesz J, Fork DC (eds) (1986) Light emission by plants and bacteria. Academic Press, New York

Guadagno CR, Virzo De Santo A, D'Ambrosio N (2010) A revised energy partitioningapproach to assess the yields of non-photochemical quenching components. Biochim Biophys Acta 1797:525–530

Gururani MA, Venkatesh J, Ganesan M, Strasser RJ, Han Y, Kim JI, Lee HY, Song PS (2015) In vivo assessment of cold tolerance through chlorophyll a fluorescence in transgenic Zoysiagrass expressing mutant phytochrome A. PLoS ONE 10(5):e0127200

Guy CL (1990) Cold acclimation and freezing stress tolerance: Role of protein metabolism. Annu Rev Plant Physiol Plant Mol Biol 4:187–223

Hacker J, Spindelbock JP, Neuner G (2008) Mesophyll freezing and effects of freeze dehydration visualized by simultaneous measurement of IDTA and differential imaging chlorophyll fluorescence. Plant Cell Environ 31:1725–1733

Hannah MA, Wiese D, Freund S, Fiehn O, Heyer AG, Hincha DK (2006) Natural genetic variation of freezing tolerance in Arabidopsis. Plant Physiol 142:98–112

Hasdai M, Weiss B, Levi A, Samach A, Porat R (2006) Differential responses of Arabidopsis ecotypes to cold, chilling and freezing temperatures. Ann Appl Biol 148:113–120

Hendrickson L, Furbank RT, Chow WS (2004) A simple alternative approach to assessing the fate of absorbed light energy using chlorophyll fluorescence. Photosynth Res 82:73–81

Hikosaka K, Ishikawa K, Borjigidai A, Muller O, Onoda Y (2006) Temperature acclimation of photosynthesis: mechanisms involved in the changes in temperature dependence of photosynthetic rates. J Exp Bot 57:291–302

Holub O, Seufferheld MJ, Gohlke C, Govindjee, Heiss GJ, Clegg RM (2007) Fluorescence lifetime imaging microscopy of *Chlamydomonas reinhardtii*: non-photochemical quenching mutants and the effect of photosynthetic inhibitors on the slow chlorophyll fluorescence transient. J Microsc 226:90–120

Horton P (2012) Optimization of light harvesting and photoprotection: molecular mechanisms and physiological consequences. Phil Trans R Soc B 367:3455–3465

Humplík JF, Lazár D, Fürst T, Husičková A, Hýbl M, Spíchal L (2015) Automated integrative high-throughput phenotyping of plant shoots: a case study of the cold-tolerance of pea (*Pisum sativum L.*). Plant Methods 11:20

Huner NPA, Öquist G, Sarhan F (1998) Energy balance and acclimation to light and cold. Trends Plant Sci 3:224–230

Joliot P, Johnson GN (2011) Regulation of cyclic and linear electron flow in higher plants. Proc Natl Acad Sci USA 108:13317–13322

Joliot P, Joliot A (2002) Cyclic electron transfer in plant leaf. Proc Natl Acad Sci USA 99(15):10209–10214

Joliot P, Joliot A (2006) Cyclic electron flow in C3 plants. Biochim Biophys Acta 1757:362–368

Kalaji HM, Goltsev V, Bosa K, Allakhverdiev SI, Strasser RJ, Govindjee (2012) Experimental in vivo measurements of light emission in plants: A perspective dedicated to David Walker. Photosynth Res 114:69–96

Kaňa R, Govindjee (2016) Role of ions in the regulation of light-harvesting. Front Plant Sci 7:1849

Kaňa R, Kotabová E, Komárek O, Šedivá B, Papageorgiou GC, Govindjee, Prášil O (2012) The slow S to M fluorescence rise in cyanobacteria is due to a state 2 to state 1 transition. Biochim Biophys Acta 1817:1237–1247

Khanal N, Bray G, Grisnich A, Moffatt B, Gray G (2017) Differential mechanisms of photosynthetic acclimation to light and low temperature in Arabidopsis and the extremophile *Eutrema salsugineum*. Plants. https://doi.org/10.3390/plants6030032

Knaupp M, Mishra KB, Nedbal L, Heyer AG (2011) Evidence for a role of raffinose in stabilizing photosystem II during freeze-thaw cycles. Planta 234:477–486

Kodru S, Malavath T, Devadasu E, Nellaepalli S, Subramanyam R, Govindjee (2015) The slow S to M rise of chlorophyll *a* fluorescence induction reflects transition from state 2 to state 1 in the green alga *Chlamydomonas reinhardtii*. Photosynth Res 125:219–231

Kramer DM, Evans JR (2011) The importance of energy balance in improving photosynthetic productivity. Plant Physiol 155:70–78

Kramer DM, Johnson G, Kiirats O, Edwards GE (2004) New fluorescence parameters for the determination of QA redox state and excitation energy fluxes. Photosynth Res 79:209–218

Lamb JJ, Rokke G, Hohmann-Marriott MF (2018) Chlorophyll fluorescence emission spectroscopy of oxygenic organisms at 77 K. Photosynthetica 56(1):105–124

Lazár D (1999) Chlorophyll a fluorescence induction. Biochim Biophys Acta 1412:1–28

Lazár D (2015) Parameters of photosynthetic energy partitioning. J Plant Physiol 175:131–147

Leegood RC, Edwards GE (1996) Carbon metabolism and photorespiration: temperature dependence in relation to other environmental factors. In: Baker NR (ed) Photosynthesis and the environment. Kluwer Academic Publishers, Dordrecht, pp 191–221

Lukas V, Mishra A, Mishra KB, Hajslova J (2013) Mass spectrometry-based metabolomic fingerprinting for screening cold tolerance in *Arabidopsis thaliana* accessions. Anal Bioanal Chem 405(8):2671–2683

Malenovský Z, Mishra KB, Zemek F, Rascher U, Nedbal L (2009) Scientific and technical challenges in remote sensing of plant canopy reflectance and fluorescence. J Exp Bot 60:2987–3004

Marečková M, Barták M (2016) Effects of short-term low temperature stress on chlorophyll fluorescence transients in Antarctic lichen species. Czech Polar Reports 6(1):54–65

Martindale W, Leegood RC (1997) Acclimation of photosynthesis to low temperature in *Spinacia oleracea* L.II. Effects of nitrogen supply. J Exp Bot 48:1873–1880

Maxwell K, Johnson GN (2000) Chlorophyll fluorescence—a practical guide. J Exp Bot 51:659–668

Mishra A, Mishra KB, Höermiller II, Heyer AG, Nedbal L (2011) Chlorophyll fluorescence emission as a reporter on cold tolerance in *Arabidopsis thaliana* accessions. Plant Signal Behav 6:301–310

Mishra A, Heyer AG, Mishra KB (2014) Chlorophyll fluorescence emission can screen cold tolerance of cold acclimated *Arabidopsis thaliana* accessions. Plant Methods 10:38

Mishra A, Hájek J, Tuháčková T, Barták M, Mishra KB (2015) Features of chlorophyll fluorescence transients can be used to investigate low temperature induced effects on photosystem II of algal lichens from polar regions. Czech Polar Reports 5(1):99–111

Mishra KB, Mishra A, Klem K, Govindjee (2016a) Plant phenotyping: A perspective. Indian J Plant Physiol 21(4):514–527

Mishra KB, Mishra A, Novotná K, Rapantová B, Hodaňová P, Urban O, Klem K (2016b) Chlorophyll *a* fluorescence, under half of the adaptive growth-irradiance, for high-throughput sensing of leaf-water deficit in *Arabidopsis thaliana* accessions. Plant Methods 12:46

Mohanty P, Govindjee (1974) The slow decline and subsequent rise of chlorophyll fluorescence transients in intact algal cells. Plant Biochem J 1:78–106

Mohanty P, Papageorgiou GC, Govindjee (1971) Fluorescence induction in the red alga *Porphyridium cruentum*. Photochem Photobiol 14:667–682

Mohanty P, Suleyman IA, Murata N (2007) Application of low temperatures during photoinhibition allows characterization of

individual steps in photodamage and the repair of photosystem II. Photosynth Res 94:217–224
Müller P, Li XP, Niyogi K (2001) Non-photochemical quenching. A response to excess light energy. Plant Physiol 125:1558–1566
Munday JC, Govindjee (1969) Light-induced changes in the fluorescence yield of chlorophyll a in vivo: III. The dip and peak in the fluorescence transient of *Chlorella pyrenoidosa*. Biophys 9:1–21
Murchie EH, Niyogi KK (2011) Manipulation of photoprotection to improve plant photosynthesis. Plant Physiol 155:86–92
Öquist G, Greer DH, Ögren E (1987) Light stress at low temperature. In: Kyle DJ, Osmond CB, Arntzen CJ (eds) Topics in Photosynthesis. Elsevier, Amsterdam, pp 67–87
Ort DR, Baker NR (2002) A photoprotective role for O_2 as an alternative electron sink in photosynthesis? Curr Opin Plant Biol 5:193–198
Ort DR, Merchant SS, Alric J, Barkan A, Blankenshiph RE et al (2015) Redesigning photosynthesis to sustainably meet global food and bioenergy demand. Proc Natl Acad Sci USA 112(28):8529–8536
Oxborough K (2004) Imaging of chlorophyll *a* fluorescence: theoretical and practical aspects of an emerging technique for the monitoring of photosynthetic performance. J Exp Bot 55:1195–1205
Pandey JK, Gopal R (2012) Dimethoate-induced slow S to M chlorophyll a fluorescence transient in wheat plants. Photosynthetica 50:630–634
Papageorgiou GC, Govindjee (1968a) Light-induced changes in the fluorescence yield of chlorophyll *a* in vivo I. *Anacystis nidulans*. Biophys J 8:1299–1315
Papageorgiou GC, Govindjee (1968b) Light-induced changes in the fluorescence yield of chlorophyll *a* in vivo. II. Chlorella pyrenoidosa. Biophys J 8:1316–1328
Papageorgiou GC, Govindjee (eds) (2004) Chlorophyll *a* fluorescence: a signature of photosynthesis. Advances in Photosynthesis and Respiration, vol 19. Springer, Dordrecht
Papageorgiou GC, Govindjee (2011) Photosynthesis II fluorescence: slow changes-scaling from the past. J Photochem Photobiol B 104:258–270
Papageorgiou GC, Tsimilli-Michael M, Stamatakis K (2007) The fast and slow kinetics of chlorophyll *a* fluorescence induction in plants, algae and cyanobacteria: A viewpoint. Photosynth Res 94:275–290
Pospíšil P, Skotnica J, Nauš J (1998) Low and high temperature dependence of minimum F-O and maximum F-M chlorophyll fluorescence in vivo. Biochim Biophys Acta 1363:95–99
Roháček K (2010) Method for resolution and quantification of components of the non-photochemical quenching (qN). Photosynth Res 105:101–113
Roháček K, Soukupova J, Bartak M (2008) Chlorophyll fluorescence: A wonderful tool to study plant physiology and plant stress. Plant Cell Compartments– Selected Topics, Editor: Benoit Schoefs. Chapter 3: 41–104. Research Signpost, Trivandrum, India. ISBN: 978-81-308-0104-9
Ruban AV, Berera R, Ilioaia C, Van Stokkum IH, Kennis JT, Pascal AA, Van Amerongen H, Robert B, Horton P, Van Grondelle R (2007) Identification of a mechanism of photoprotective energy dissipation in higher plants. Nature 450:575–578
Sage RF, Kubien DS (2007) The temperature response of C-3 and C-4 photosynthesis. Plant Cell Environ 30:1086–1106
Sane PV, Ivanov AG, Hurry V, Huner NP, Oquist G (2003) Changes in the redox potential of primary and secondary electron-accepting quinones in photosystem II confer increased resistance to photoinhibition in low-temperature-acclimated Arabidopsis. Plant Physiol 132(4):2144–2151
Savitch LV, Gray GR, Huner NPA (1997) Feedback-limited photosynthesis and regulation of sucrose-starch accumulation during cold acclimation and low temperattre stress in a spring and winter wheat. Planta 201:18–26
Schmid KJ, Sorensen TR, Stracke R, Torjek O, Altmann T, Mitchell-Olds T, Weisshaar B (2003) Large-scale identification and analysis of genome-wide single-nucleotide polymorphisms for mapping in Arabidopsis thaliana. Genome Res 13:1250–1257
Seaton GGR, Walker DA (1990) Chlorophyll fluorescence as a measure of photosynthetic carbon assimilation. Proc Royal Soc: Biol Sci 242(1303):29–35
Shikanai T (2007) Cyclic electron transport around photosystem I:genetic approaches. Annu Rev Plant Biol 58:199–217
Sivak MN, Dietz J-J, Heber U, Walker DA (1985a) The relationship between light-scattering and chlorophyll a fluorescence during oscillation in photosynthesis carbon assimilation. Arch Biochem Biophys 237:513–519
Sivak MN, Heber U, Walker DA (1985b) Chlorophyll *a* fluorescence and light-scattering displayed be leaves during induction of photosynthesis. Planta 163:419–423
Smallwood M, Bowles DJ (2002) Plants in a cold climate. Philos Trans Roy Soc B 357:831–846
Stirbet A, Govindjee (2011) On the relation between the Kautsky effect (chlorophyll a fluorescence induction) and Photosystem II: Basics and applications of the OJIP fluorescence transient. J Photochem Photobiol B: Biol 104:236–257
Stirbet A, Govindjee (2012) Chlorophyll a fluorescence induction: A personal perspective of the thermal phase, the J-I-P rise. Photosynth Res 113:15–61
Stirbet A, Govindjee (2016) The slow phase of chlorophyll *a* fluorescence induction in silico: Origin of the S-M fluorescence rise. Photosynth Res 130:193–213
Stirbet A, Lazár D, Kromdijk G (2018) Chlorophyll a fluorescence induction: Can just a one-second measurement be used to quantify abiotic stress responses? Photosynthetica 56(1):86–104
Strand Å, Hurry V, Henkes S, Huner N, Gustafsson P, Gardeström P, Stitt M (1999) Acclimation of Arabidopsis leaves developing at low temperatures. Increasing cytoplasmic volume accompanies increased activities of enzymes in the Calvin Cycle and in the sucrose-biosynthesis pathway. Plant Physiol 119:1387–1397
Strasser RJ, Srivastava A, Govindjee (1995a) Polyphasic chlorophyll *a* fluorescence transient in plants and cyanobacteria. Photochem Photobiol 61:32–42
Strasser RJ, Srivastava A, Govindjee (1995b) Polyphasic chlorophyll *a* fluorescence transient in plants and cynobecteria. Photochem Photobiol 61:32–42
Telfer A, Nicolson J, Barber J (1976) Cation control of chloroplast structure and chlorophyll *a*fluorescence yield and its relevance to the intact chloroplast. FEBS Lett 65(1):77–83
Thomashow MF (2010) Molecular basis of plant cold acclimation: insight gained from studying the CBF cold response pathway 1. Plant Physiol 154:571–577
Tóth SZ, Schansker G, Strasser RJ (2007) A non-invasive assay of the plastoquinone pool redox state based on the OJIP-transient. Photosynth Res 93:193–203
Triantaphylidès C, Havaux M (2009) Singlet oxygen in plants: production, detoxification and signaling. Trends Plant Sci 14(4):219–228
Tyystjärvi E (2013) Photoinhibition of photosystem II. Int Rev Cell Mol Biol 300:243–303
Tyystjärvi E, Aro E-M (1996) The rate constant of photoinhibition, measured in lincomycin-treated leaves, is directly proportional to light intensity. Proc Natl Acad Sci USA 93:2213–2218
Urban O, Sprtova M, Kosvancova M, Tomaskova I, Lichtenthaler HK, Marek MV (2008) Comparison of photosynthetic induction and transient limitations during the induction phase in young and mature leaves from three poplar clones. Tree Physiol 28:1189–1197

Walker DA (1981) Secondary fluorescence kinetics of spinach leaves in relation to the onset of photosynthetic carbon assimilation. Planta 153:273–278

Walters RG, Horton P (1991) Resolution of components of non-photochemical chlorophyll fluorescence quenching in barley leaves. Photosynth Res 27:121–133

Walters RG, Ruban AV, Horton P (1996) Identification of proton-active residues in a higher plant light-harvesting complex. Proc Natl Acad Sci USA 93:14204–14209

Wanner LA, Junttila O (1999) Cold-induced freezing tolerance in Arabidopsis. Plant Physiol 120:391–399

Yamagishi A, Satoh K, Katoh S (1978) Fluorescence induction in chloroplasts isolated from the green alga *Bryopsis maxima*. III. A fluorescence transient indicating proton gradient across the thylakoid membrane. Plant Cell Physiol 19:17–25

Yun JG, Hayashi T, Yazawa S, Yasuda Y, Katoh T (1997) Degradation of photosynthetic activity of *Saintpaulia* leaf by sudden temperature drop. Plant Sci 127:25–38

Zhang S, Scheller HV (2002) Photoinhibition of Photosystem I at chilling temperature and subsequent recovery in *Arabidopsis thaliana*. Plant Cell Physiol 45:1595–1602

Affiliations

Kumud B. Mishra[1,2] · Anamika Mishra[1] · Jiří Kubásek[1] · Otmar Urban[1] · Arnd G. Heyer[3] · Govindjee[4]

Anamika Mishra
mishra.a@czechglobe.cz

Jiří Kubásek
jirkak79@gmail.com

Otmar Urban
urban.o@czechglobe.cz

Arnd G. Heyer
arnd.heyer@bio.uni-stuttgart.de

Govindjee
gov@illinois.edu

[1] Global Change Research Institute, Czech Academy of Sciences, Bělidla 986/4a, 603 00 Brno, Czech Republic

[2] Department of Experimental Biology, Masaryk University, Kamenice 5, 625 00 Brno, Czech Republic

[3] Department of Plant Biotechnology, Institute of Biomaterials and Biomolecular Systems, University of Stuttgart, Pfaffenwaldring 57, 70567 Stuttgart, Germany

[4] Department of Plant Biology, Department of Biochemistry and Center for Biophysics and Quantitative Biology, University of Illinois at Urbana-Champaign, Urbana, IL 61801, USA